

Union College

Union | Digital Works

Honors Theses

Student Work

6-2020

Groundwater isotopes across scales: continent-wide modeling and local field characterization

Jaclyn Gehring

Follow this and additional works at: <https://digitalworks.union.edu/theses>



Part of the [Geology Commons](#), [Hydrology Commons](#), [Sustainability Commons](#), and the [Water Resource Management Commons](#)

Recommended Citation

Gehring, Jaclyn, "Groundwater isotopes across scales: continent-wide modeling and local field characterization" (2020). *Honors Theses*. 2385.

<https://digitalworks.union.edu/theses/2385>

This Open Access is brought to you for free and open access by the Student Work at Union | Digital Works. It has been accepted for inclusion in Honors Theses by an authorized administrator of Union | Digital Works. For more information, please contact digitalworks@union.edu.

**Groundwater isotopes across scales: continent-wide modeling and local field
characterization**

By

Jaclyn Gehring

* * * * *

**Submitted in Partial Fulfillment
of the Requirements for
Honors in the Department of Geology**

UNION COLLEGE

June, 2020

ABSTRACT

GEHRING, JACLYN. Groundwater isotopes across scales: continent-wide modeling and local field characterization. Department of Geology, June 2020.

THESIS ADVISOR: Mason Stahl

Groundwater is one of the world's most important natural resources. The use of stable water isotopes ($\delta^2\text{H}$ and $\delta^{18}\text{O}$) as natural tracers through the water cycle has provided a unique observational technique for characterizing hydrological processes and establishing connections between water distribution systems and their respective environmental sources. Groundwater contains information about the timing and efficiency of recharge, allowing for the use of isotopes to understand the physical hydrology and climatic influences on such processes in places with groundwater isotope measurements. We estimate the seasonal recharge proportion and efficiency at thousands of locations across the U.S., and interpret the climatic and environmental influences responsible for our findings. Results along coastal California suggest fog drip contributes to groundwater recharge and necessitates additional research in areas where this process may be an important source of recharge to aquifers. To combat pre-existing limitations of the lack of groundwater data across all locations in the United States, a predictive model for groundwater isotopes was developed across the contiguous U.S. using a random forest model based on environmental parameters. We find evident spatial coherence in the model predictions, generally mirroring the signal of isotopes of precipitation, and highlight the potential for its application across hydrology and ecology.

In addition, to demonstrate the applicability and versatility of groundwater isotopes, we investigated the local municipal water supply in Schenectady, New York, to understand the source and timing of aquifer recharge. The Schenectady municipal well-field is sited less than a

kilometer from the Mohawk River, making the interaction between surface water and groundwater highly complex and seasonally dependent. Schenectady tap water, which is drawn from local groundwater, and Mohawk River were collected at regular intervals and analyzed in the Union College Stable Isotope Laboratory for stable isotopes of hydrogen and oxygen. The seasonal signal of isotopes can be approximated by sine waves, and the phase and amplitude of these signals can be used to calculate the average linear velocity (3.53 m/day) of the water moving into the aquifer and fraction of young water (57% < 2.7 months) in the local groundwater. Our results highlight the connection between the Mohawk River and the aquifer in the vicinity of the Schenectady well-field, and motivates further research to characterize the potential for vulnerabilities. Thus, this study not only provides an isoscape to detail the spatial distribution of isotopes regionally, but also demonstrates how we can leverage our understanding of isotopes for insight into the chemical and physical hydrology in a local water system.

ACKNOWLEDGEMENTS

Thank you to Mason Stahl for being a kind, brilliant, and supportive advisor and mentor throughout my time at Union. I am grateful for his constant enthusiasm and advice in everything academics, research, and life for the past few years. He has truly bolstered my experience at Union by guiding my passion in hydrology, and I would not be the student and researcher I am without him; I am excited to continue to work with him on future projects.

This project has been made possible through the Potter and Davenport Summer Research Fellowships and Union Student Research Grants, as well as the support from the Union College Geology Department. Thank you to Anouk Verheyden-Gillikin, David Gillikin, and Madelyn Miller in the Stable Isotope Laboratory for their help analyzing our water samples. I was also very fortunate to be able to work with Yusuf Jameel for a part of this project, who has provided invaluable encouragement and insight.

Lastly, thank you to my family and friends for their love and support throughout my time at Union College; I would not be where I am today without you all!

TABLE OF CONTENTS

1	<i>Introduction</i>	1
1.1	STABLE ISOTOPE THEORY	2
1.2	STABLE ISOTOPES IN HYDROLOGY	4
1.3	THESIS OVERVIEW	11
1.3.1	Characterizing Hydrologic Processes using Groundwater Isotopes	12
1.3.2	Development of a National Groundwater Isoscape.....	14
1.3.3	Surface Water and Groundwater Interaction Along the Mohawk River	16
2	<i>Characterizing Hydrologic Processes using Groundwater Isotopes</i>	20
2.1	BACKGROUND	21
2.2	METHODOLOGY	22
2.2.1	Data Acquisition.....	22
2.2.2	Calculating Recharge Proportions and Efficiency	24
2.3	RESULTS AND DISCUSSION	27
2.3.1	Regional Patterns in Groundwater Isotopes.....	27
2.3.2	Seasonal Recharge Efficiencies	34
2.3.3	Seasonal Recharge Proportions.....	36
2.3.4	West Coast Processes	37
2.4	CONCLUSIONS	39
3	<i>Development of a National Isoscape</i>	40
3.1	BACKGROUND	41
3.2	METHODOLOGY	43
3.2.1	Kriging Approach.....	43
3.2.2	Random Forest Model	46
3.3	RESULTS	48
3.3.1	Kriging Approach.....	48
3.3.2	Random Forest Model	49

3.4	DISCUSSION	52
3.5	CONCLUSIONS	54
4	<i>Surface Water and Groundwater Interaction Along the Mohawk River</i>	56
4.1	BACKGROUND	57
4.1.1	Geologic Setting.....	58
4.1.2	Water Supply.....	60
4.2	METHODOLOGY	62
4.2.1	Field Methodology	62
4.2.2	Laboratory Methodology	62
4.2.3	Hydrologic Analysis.....	63
4.3	RESULTS	67
4.4	DISCUSSION	71
4.4.1	Fraction Young and Mean Transit Timing	71
4.4.2	Physical Hydrology	73
4.5	CONCLUSIONS	75
5	<i>Conclusions</i>	77
5.1	SUMMARY	78
5.2	FUTURE RESEARCH	79
6	<i>References</i>	80

1 Introduction

1.2 STABLE ISOTOPE THEORY

Advances in technology have promoted the expansion of isotope analyses and applications throughout the past century (Bowen et al., 2019). Stable isotopes of oxygen and hydrogen are widely used throughout the sciences for understanding biogeochemical cycles, contaminant cycling, and the reconstruction of paleoclimates. The existence of stable isotopes was discovered in 1913, when J.J. Thomson realized some atoms of neon gas consisted of higher mass than the others. Isotopes exist as a result of the neutron variation of an element; thus, for a given element, isotopes have the same number of protons but varying numbers of neutrons (Clark, 2015; Sharp, 2017). Stable isotopes describe atoms of an element which do not decay over time (or do not decay quickly through time; Clark and Fritz, 1997). Despite this difference in isotopes, the nature of chemical reactions does not change; however, during physical and geochemical reactions, the slight difference in mass causes isotopes to behave differently, as the variation in energy partitions isotopes—heavy and light—on opposite sides of the reaction (Daansgard, 1964; Clark, 2015). Stable isotopes are expressed by their abundance ratio, reflecting a given concentration relative to the most abundant isotope at a given time (Clark and Fritz, 2013).

Water cycle research has depended on stable isotope ratios of hydrogen and oxygen, as they allow for the tracking of water sources and hydrological processes that influence these sources (Bowen et al., 2019). The two naturally occurring and stable isotopes of hydrogen are ^1H and ^2H . The most common isotope of hydrogen is protium (^1H), with an abundance of more than 99.98%. Deuterium (^2H or D) consists of one proton and one neutron, and has an abundance of approximately 0.00156%; the atomic mass of deuterium is 2.014, which causes it to react more slowly than hydrogen (^1H) as it enters into chemical reactions. Oxygen-18 (^{18}O) is

an isotope of the common oxygen-16 (^{16}O); rarer is the presence of the isotope ^{17}O , although it records similar information to that of ^{18}O (Bowen et al., 2019). The abundance of ^{16}O is 99.762%, while ^{18}O exists with an abundance of 0.20%.

Ratios of hydrogen isotopes and oxygen isotopes are widely used in water cycle studies. $\delta^2\text{H}$ describes the ratio of ^2H to ^1H , and is typically used in hydrologic and ecologic applications (Coplen, 1995; Sharp, 2017; Vander Zanden et al., 2016). $\delta^{18}\text{O}$ describes the ratio of ^{18}O to ^{16}O , and is typically used in studies of paleoclimatology and hydrology (Sharp, 2017; Vander Zanden et al., 2019; Bowen et al., 2019). The relative abundance of water isotopes—including ^1H , ^2H , ^{16}O , and ^{18}O —vary throughout the hydrologic cycle (Bowen et al., 2019).

Water molecules are formed by the combination of hydrogen atoms (^1H and ^2H) and oxygen atoms (^{16}O , ^{17}O , or ^{18}O); thus, there are nine isotopologues of water (Clark, 2015). The most abundant isotopologues of water in nature include H_2^{16}O , H_2^{18}O , H_2^{17}O , and HD^{16}O , with measurable abundances of 99.731%, 0.199978%, 0.037888%, and 0.03146%, respectively (Galewsky et al., 2016). As water molecules travel through the hydrological cycle, the various isotopic compositions of these isotopologues cause differentiation in the partitioning between their vapor, liquid, and solid phases. This distinguishing isotopic signature is the basis for stable isotope analysis in hydrology (Clark and Fritz, 1997; Kirshan, 2015).

Measurements of isotopic values are expressed as a ratio of the concentrations of the heavy isotope compared to the light isotope. This ratio is expressed relative to the international standard (as defined by the International Atomic Energy Agency, or IAEA) for the isotopic composition of water; the Vienna Standard Mean Ocean Water (VSMOW) standard for D/H is 155.95×10^{-6} , and the standard for $^{18}\text{O}/^{16}\text{O}$ is 2005.2×10^{-6} (Galewsky et al., 2016). The δ

notation (expressed in units of per mil) describes the isotopic composition of a given ratio of a sample (R_{Sample}):

$$\delta = \frac{R_{\text{Sample}} - R_{\text{Standard}}}{R_{\text{Standard}}} \times 1000,$$

where R_{Standard} , for a water sample, is the respective value for a standard of VSMOW. Samples with more negative values have fewer heavy isotopes, and are thus described as being “more depleted” in heavy isotopes. Samples with higher, more positive values are typically described as being “heavier,” or “enriched” in the heavy isotope.

1.3 STABLE ISOTOPES IN HYDROLOGY

There are naturally occurring isotopes of major elements which exist at the earth’s surface. The foundation of isotope hydrology, perhaps one of the earliest applications of stable isotope chemistry, was established by Harmon Craig in 1961, when he published early global measurements of $\delta^{18}\text{O}$ and $\delta^2\text{H}$ for freshwater (Bowen et al., 2019). Climatic influences on isotopes were first established in 1964 Willi Dansgaard, when he correlated values of $\delta^{18}\text{O}$ and $\delta^2\text{H}$ with air temperature for given regions (Dansgaard, 1964; Clark, 2015). Because stable isotopes of water are naturally occurring, conservative within a water body, and do not decay overtime, isotopes in water are useful for understanding the global water cycle, which is essential for addressing environmental issues regarding water quality, availability, and transport (Bowen and Good, 2015; Sharp, 2017).

The thermodynamics of equilibrium and kinetic reactions facilitates the partitioning of isotopes in the environment and dictates their physio-chemical behavior. Although there is no chemical difference in isotope substitution, there are changes in vibrational frequency (Clark, 2015). Equilibrium fractionation is mass-dependent and reversible (Sharp, 2017). Equilibrium

isotope effects distribute isotopes in a system such that the total energy of the system is minimized. The source of fractionation is caused by differences in vibrational energy between heavier and lighter isotopes; slightly differing free energies for atoms of different atomic weight dictates such behavior. The equilibrium fractionation between two phases is determined by the bond strength, such that heavier isotopes are concentrated where the bonds are strongest (Sharp, 2017). Thus, a heavier isotope would equilibrate into the phase in which it is most stable—where the bonds are strongest. For example, heavier water isotopes are preferentially incorporated into the liquid phase, while lighter isotopes preferentially remain in the vapor phase. Additionally, equilibrium isotope effects are temperature-dependent, indicating fractionation is larger at lower temperatures (Sharp, 2017). Equilibrium processes are responsible for much of the natural variation in isotopes (Bowen et al., 2019).

Kinetic isotope effects describe the change in reaction rate of a chemical reaction due to the isotopic replacement of a reactant. Differences in velocities occurring because of slight differences in mass leads to variety in isotope fractionation (Clark, 2015). These effects are often associated with processes such as evaporation and diffusion, as they are fast and irreversible (Sharp, 2017; Bowen et al., 2019). Isotopically light molecules preferentially diffuse out of a system, leaving the reservoir enriched in the heavier isotope (Clark, 2015). An example of such an effect is the diffusion-based fractionation between water and vapor, as lighter isotopes typically react more quickly than heavier isotopes. As a result, the vapor phase preferentially incorporates the lighter isotopes (Bowen et al., 2019). Thus, kinetic isotope effects describe the reaction mechanisms.

The distribution of isotopes in water is controlled by the fractionation and distillation of isotopes (Figure 1).

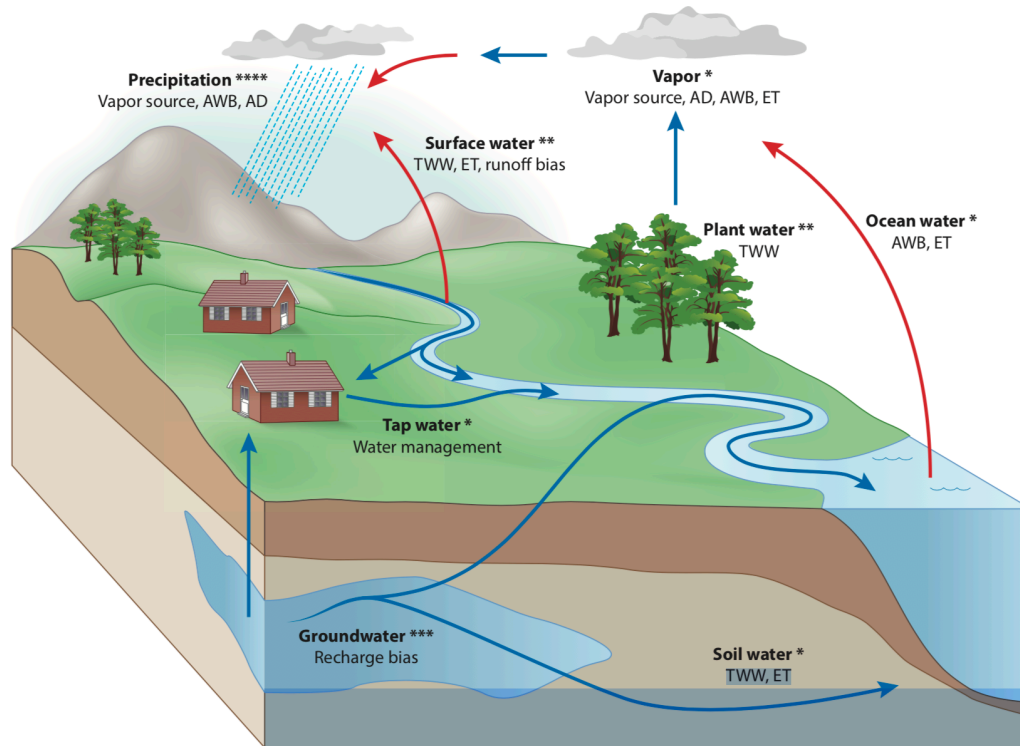


Figure 1. Schematic of isotopes of water as they move through the hydrologic cycle (Bowen et al., 2019).

Fractionation and distillation are used to describe partitioning, relative to processes which affect the relative abundance of isotopes. Oxygen and hydrogen isotopes are strongly fractionated as they move through the hydrological cycle (Sharp, 2017; Bowen et al., 2019). The fractionation of isotopes in water are predictable and well-understood, allowing for the interpretation of hydrologic processes (Clark, 2015). The large fractionation, associated with evaporation and condensation, is temperature dependent and originates from kinetic and equilibrium effects (Sharp, 2017). Processes which affect the distribution of isotopes through the hydrologic cycle include evaporation, condensation, recharge mixing, and gas-water exchanges.

The Global Meteoric Water Line (GMWL) describes the relationship between average hydrogen and oxygen isotopes in precipitation, and is useful for understanding the hydrologic

cycle. The GMWL is defined by the following equation because of the nearly linear relationship between oxygen and hydrogen isotopes of precipitation:

$$\delta^2\text{H} = 8 * \delta^{18}\text{O} + 10,$$

where the intercept reflects kinetic effects if the evaporation is not at 100% humidity (Craig, 1961). Deuterium excess (d-excess) is defined as $d = \delta^2\text{H} - 8 * \delta^{18}\text{O}$. The d-excess parameter results from different evaporation rates for the various isotopologues of water, as the kinetic isotope effect has a larger influence on deuterium isotopes compared to oxygen isotopes (Dansgaard, 1964). In precipitation, the average value for d-excess globally is 10‰. The Local Meteoric Water Line (LMWL) reflects the isotopes of precipitation at a single location, and differences can reveal the influences of hydrologic processes that drive fractionation (Dansgaard, 1964). Because of the complex exchange between the surface and the atmosphere, deviations from the GMWL (differences between the slope of 8 and the d-excess of 10‰) provide insight into nonequilibrium processes, including evapotranspiration and moisture source (Dansgaard, 1964). Moisture sources generated from vapor at less than 100% humidity will subsequently rain out with a d-excess greater than the original source; thus, deuterium excess is generally interpreted as a proxy for the source of moisture. An important reference line and tool in isotope hydrology, the GMWL helps to provide insight into the evolution process of surface water and groundwater.

The main factors affecting isotopes of precipitation—and, subsequently, natural waters from which these isotopic variations are derived—include temperature, continentality, and latitude. Isotopes of precipitation, of which the ocean is understood to be the dominant moisture source, follow a natural sequence of fractionation (Clark, 2015). Variations in isotopic compositions occur through time, seasonally, or between storm events (Sharp, 2017).

The evolution of a system with multiple phases is captured by Rayleigh fractionation or distillation, which describes the isotopic enrichment or depletion of water molecules as they move between reservoirs through equilibrium processes (Clark, 2015; Sharp, 2017). This type of evolution occurs for environmental processes, including the depletion of isotopes in a vapor mass as a cause of rainout (Figure 2).

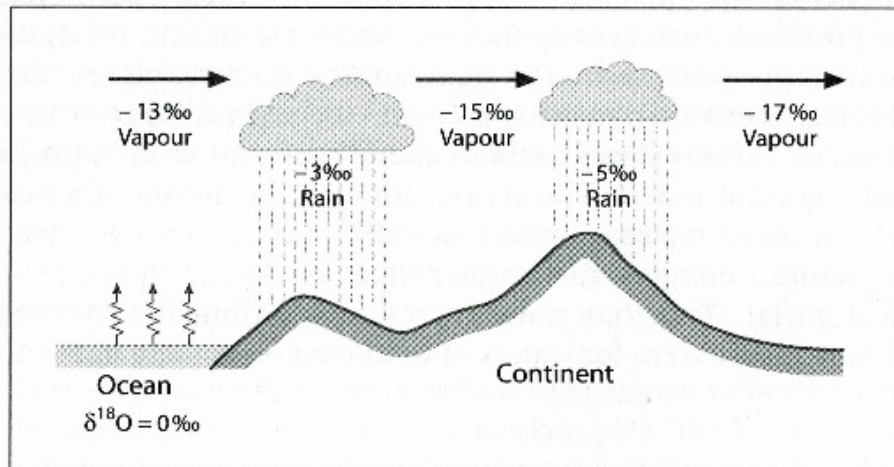


Figure 2. A schematic of the physical fractionation of isotopes by evaporation, precipitation, and precipitation amount (Sharp, 2017). Evaporation favors the light isotope of oxygen, resulting in a lighter isotopic value in the vapor. As vapor condenses into rain, the heavier isotope is preferentially rained out, such that precipitation is enriched in the heavier isotope. Moving away from the vapor source, values become depleted as each evolution is lighter due to heavier isotopes being removed by precipitation.

As a reactant is removed from the system, the product is limited because there is no exchange after the separation; each phase of the evolution of vapor occurs in equilibrium with the previous phase, but is removed from the system as precipitation (Sharp, 2017). Rayleigh distillation describes how the isotopic composition of a system evolves as one phase is removed under equilibrium conditions, controlled by the fractionation factor, which is temperature dependent (Clark and Fritz, 1997). Much of the natural variation in precipitation isotopes globally is thought to be governed by the Rayleigh distillation model (Bowen et al., 2019).

The relationship between stable isotopes and temperature is perhaps the foundation underlying isotope hydrology and its applications to paleoclimatology (Bowen et al., 2019). Temperature, varying temporally and spatially, controls the fractionation of isotopes in precipitation, as temperature-based mechanisms drive changes in isotopes (Clark and Fritz, 1997). The positive correlation between temperature and isotopes of oxygen and hydrogen in precipitation suggests an increase in temperature causes intense evaporation, resulting in the rainout of heavier isotopes (Dansgaard, 1964; Clark, 2015). As temperature changes with seasons, seasonal effects become apparent in isotopic compositions; isotopes are typically depleted (become more negative) as seasonality increases (Dansgaard, 1964). Seasonal differences in isotopes are strongest when there are large seasonal differences in temperature, while areas experiencing minimal variation in seasonal temperatures typically experience minimal differences in seasonality.

Isotopic composition of vapor is also controlled by the proximity to marine waters; as a result, the insulation of oceanic influences from the interiors of a continent leads to a depletion in precipitation isotopes. The degree of continentality is a function of temperature ranging between seasons, increasing with distance from the coast and latitude. Land masses force precipitation from vapor masses, causing the evolving vapor to move across the continent (away from the source). Seasonality is an observed effect of continentality particularly in the winter, as there is a steep temperature gradient between the ocean and interior continent (Clark, 2015). As a result, coastal regions experience isotopically enriched values of precipitation; isotopically depleted precipitation is observed near inner, colder continental regions (Clark and Fritz, 1997).

The latitude effect (linked to the relationship between isotopes and temperature) exhibits a depletion in heavier isotopes with increasing latitude, as the degree of rainout increases (Clark,

2015; Sharp, 2017). As temperature determines how much precipitation air can hold, precipitation amounts typically decrease toward the poles (high latitudes). For mid-latitude regions, this effect is observed in -0.5‰ changes per degree change of latitude; in colder regions, changes are nearly -2‰ per degree of latitude. Isotopic values from the South Pole can be used as an extreme example of the coupled effects of latitude and temperature, with values of $\delta^2\text{H}$ and $\delta^{18}\text{O}$ as low as -495‰ and -62.8‰, respectively (Sharp, 2017). This example illustrates how colder, polar regions are depleted in ^{18}O and ^2H , as lighter isotopes are precipitated at lower latitudes. Temporal variations occur in concert with the latitude effect, based on such temperature-dependence (Clark and Fritz, 1997).

Local geographic and climatic factors also influence precipitation amount and isotopic composition. The amount or rainout effect describes the significantly depleted isotopic ratios following large amounts of precipitation. Depleted values in intense precipitation events are caused by low equilibration and high humidity, or the recycling of precipitation between successive rain events (Dansgaard, 1964). Intense rainfall events are consistent with larger raindrops and higher humidity, reducing the effects of enrichment. Best observed in arid regions, the amount effect typically does not influence areas outside of the tropics, as most of the rain has already been recycled (Clark and Fritz, 1997). As a result, higher latitude regions display a weaker, negative correlation to such an effect (Kendall and Coplen, 2001). Recent studies have suggested patterns thought to be related to the rainfall-isotope variation may reflect rainfall amount and convective activity (Bowen et al., 2019). Thus, variation in rainfall and climatic activity may help to govern isotopic composition.

Topography forces a thermodynamically controlled change in isotopic ratios. With increasing altitude (and lower temperatures), isotope ratios of precipitation typically decrease.

Multiple factors contribute to this effect, including the temperature dependence of fractionation and the equilibration length of precipitation at different altitudes. The vapor pressure deficit increases with altitude, causing a decrease in saturation; rainout is driven by vapor rising (above the landscape) and cooling (Sharp, 2017). For ^{18}O , a 100-meter difference in altitude is consistent with depletion of approximately -0.15‰ to -0.5‰ (Clark and Fritz, 1997). An important effect for hydrogeological studies, the altitude effect is useful to distinguishing groundwater recharge at high altitudes from recharge at low altitudes.

Mechanistic processes and local effects are useful for understanding the isotopic compositions relative to the source (Clark, 2015). The water cycle can be better understood through the use of stable isotopes, which provide insight into hydrologic processes and pathways (Sharp, 2017). Continental and local scale variation in isotopes of precipitation must be considered for insight into recharge characteristics preserved in surface water and groundwater (Clark and Fritz, 1997). As meteoric water mixes with surface water or percolates into the ground to form groundwater, the isotopic variation is recorded, providing the basis for the detection of groundwater sources.

1.4 THESIS OVERVIEW

This thesis consists of three projects I conducted related to groundwater isotopes. In Chapter 2, I will characterize hydrologic processes using groundwater isotopes for thousands of sites across the United States. In Chapter 3, I will discuss the development of a groundwater isoscape. In Chapter 4, I will analyze local groundwater and river water samples to understand the surface water and groundwater interaction in Schenectady, New York. Chapter 5 summarizes the results of these projects and highlights the significance of using stable water

isotopes in order to improve our understanding of the physical hydrology of broad-scale and local-scale water systems.

1.4.1 Characterizing Hydrologic Processes using Groundwater Isotopes

The hydrosphere describes water on the surface of earth, governed by the hydrologic cycle—the transfer of water from land, oceans, and the atmosphere. Groundwater, stored in aquifers below the surface, is one of the world’s most important natural resources. Groundwater studies have increased in number over the past century. Technological advancements and analytical and quantitative methods have allowed for additional monitoring and measurement of groundwater resources (Bowen et al., 2019). Current environmental research has focused on the protection of groundwater resources, as groundwater represents most of the available freshwater on Earth (Knoll et al., 2019). Groundwater, in many areas of the world, provides the safest source of drinking water. In the United States, groundwater accounts for nearly 70% of water resources (Doveri et al., 2015). A consequence of economic expansion and population growth, climate change and increasing global water demands implies increasing exploitation of groundwater bodies (Doveri et al., 2015; Knoll et al., 2019). The potential for pollution, as well as overexploitation, threatens the qualitative and quantitative storages of groundwater (Doveri et al., 2015). In this way, the understanding of groundwater—including groundwater sources, recharge and recharge timing—is critical for the protection and management of water resources.

A steady increase in the number of groundwater samples containing isotopic data is observed in the United States (Figure 3).

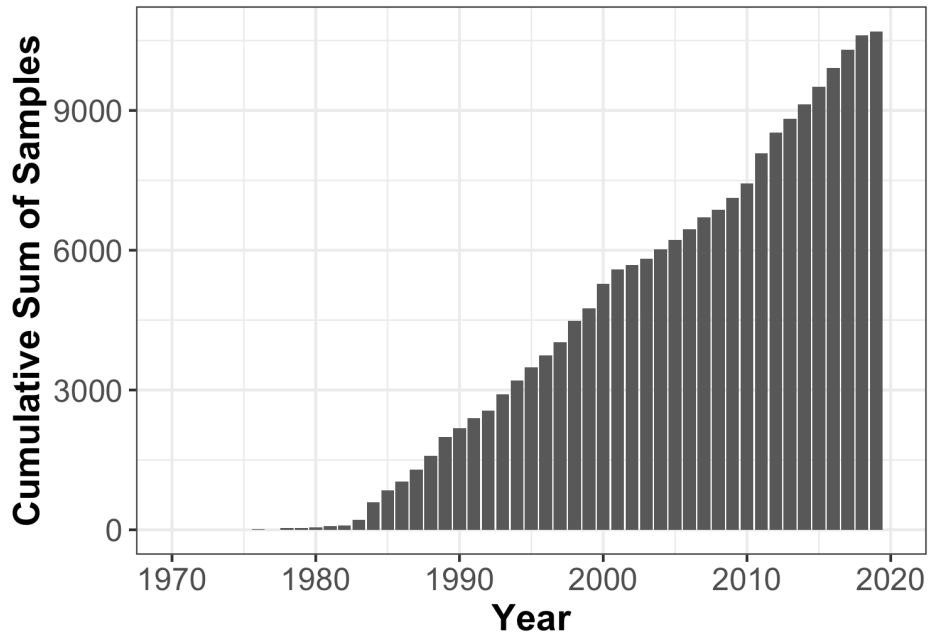


Figure 3. The steady increase in the cumulative number of groundwater samples collected by the USGS for stable water isotopes throughout the last several decades demonstrates the dramatic shift toward a greater attention to water quality information. Isotopes in water provide an effective tool for water resource management and assessment.

Understanding the movement of groundwater is important for water quality and resource management, as water sources and recharge areas can be distinguished using isotopes (Clark, 2015). Factors which impact groundwater movement include depth, sedimentology (porosity and permeability), and climatic processes. Studies of isotopes in groundwater are limited to small-scale isoscapes for small areas in the United States. The majority of relationships derived from isotopic studies originate from stream, river, and precipitation samples, as surface waters provide relatively sensitive information for movement on short-time scales (Dutton et al., 2005). In North America, the most detailed maps for isotopic composition of natural waters include those compiled by Kendall and Coplen (2001), which determine spatial coherence of isotopes in river samples and precipitation, and how these values vary geographically. Kendall and Coplen (2001) demonstrate the advantages of mapping river water for insight into regional hydrology

and climatology, as isotopic compositions of these water sources represent the dual nature of rivers in the hydrologic cycle. Applied at the same scale, groundwater data could be correlated with the average stream and river compositions to deduce recharge characteristics (Jasechko et al., 2014). The proportion and relative efficiency of groundwater recharge between seasons can be determined using groundwater data compared to isotopes of precipitation (Jasechko et al., 2014). Characterizing the importance of each season to recharge is significant, as changes to climate and subsequent environmental conditions may impact recharge timing and threaten the sustainability of our water resources.

1.4.2 Development of a National Groundwater Isoscape

Isoscapes model the spatiotemporal distribution of isotopes and provide the basis for geographic analysis (Wassenaar et al., 2009). Groundwater isoscapes have been mapped for other regions, creating a platform for additional efforts to be implemented in North America. High-resolution isoscapes for Costa Rica have been constructed using stable isotopes in groundwater, surface water, and precipitation, in order to determine dominant recharge processes in shallow aquifers (Sánchez-Murillo and Birkel, 2016). Similarly, spatial hydrogen and oxygen isotope datasets were compiled using shallow phreatic groundwaters in Mexico to understand seasonal precipitation inputs into the system (Wassenaar et al., 2009). This approach, which computes seasonally weighted precipitation values for the landscape, is applicable for countries where isotopes of precipitation and groundwater are not recorded. In such areas, information on the long-term climatic record and hydrologic processes were limited prior to using isoscapes as a water resource management tool (Sánchez-Murillo and Birkel, 2016).

Regional hydrology can be characterized by understanding spatial patterns in groundwater isotopes; despite groundwater data being readily available and applicable across a wide range of disciplines, a detailed isoscape has not been modeled for the conterminous United States. Thus, information regarding the spatial distribution of isotopes in the United States is limited to locations where samples have been collected; therefore, the lack of information on isotopic patterns in groundwater limits many studies on the modern hydrologic cycle (Bowen and Good, 2015). Understanding the degree of interaction between reservoirs in the water cycle and identifying hydrologic processes and effects responsible for isotopic signatures are useful approaches for establishing connectivity within the water cycle (Bowen and Good, 2015). Similarly, the assessment of differences in groundwater recharge between seasons aids in the understanding of groundwater sourcing (Jasechko et al., 2014). This study utilizes water quality information mainly from the USGS National Water Quality Information System (NWIS) queried using the R programming language to gather data from sites matching specific selection criteria (Cicco and Hirsch, 2014). The approaches used to estimate groundwater isotope ratios ($\delta^2\text{H}$ and $\delta^{18}\text{O}$) include a kriging method, which interpolates values using existing observations, and a random forest model, which uses environmental variables as predictors. Both approaches result in modeled isoscapes which can be used to describe patterns in groundwater isotopes across the United States. The potential for this isoscape to be used across hydrologic, ecologic, and forensic applications demonstrates the significance of groundwater isotopes for insight into hydrologic processes.

1.4.3 Surface Water and Groundwater Interaction Along the Mohawk River

Groundwater is an important freshwater resource, and thus it is important to understand the fate of groundwater; to understand the dynamic movement of water through natural systems, the geochemical properties of groundwater must be analyzed (Clark, 2015). The presence of groundwater within water-bearing rocks is called an aquifer, as this water can be readily transmitted into wells and springs (Clark, 2015). Typically, aquifers are recharged by precipitation or, to a lesser extent, surface water infiltrating underground (Clark and Fritz, 1997). In areas where groundwater is used as groundwater resources (e.g., drinking water or irrigation), aquifers can be depleted should combined groundwater withdrawals and natural discharge exceed the rate of recharge (Clark, 2015). The response of aquifers to pumping or changes in flow are can vary depending on differences in recharge for aquifers. Geologic and hydrologic conditions of the aquifer determine the level of impact (short-term or long-term) of infiltration on the aquifer (Barlow and Leake, 2012); the evaluation of groundwater resources is significant for understanding water quality and availability.

The importance of groundwater resources necessitates an investigation of groundwater recharge and recharge timing (Clark and Fritz, 1997; Bowen et al., 2019). In particular, the residence time or age of groundwater can provide insight into the vulnerability for contamination (Clark, 2015). Traditional hydrogeological methods to estimate recharge include water balance models and lysimeters, and are rooted in methodological and modelling difficulties (Clark and Fritz, 1997). Modern techniques include those that employ environmental isotopic tracer measurements to understand the response of groundwater resources; thus, environmental tracers have been used to understand groundwater flow processes, local water budgets, origin, recharge sources, and retention timing for young and old waters (McGuire et al., 2006; Kirchner, 2016).

Hydrograph separation using isotopes has allowed for the quantification of streamflow components within a watershed (Clark and Fritz, 1997). $\delta^2\text{H}$ and $\delta^{18}\text{O}$ are often used as ideal tracers for water dynamics, as isotopic compositions reflect the origin and history of groundwater prior to infiltration—whether from direct seepage from precipitation or from river or stream contribution (Bowen et al., 2019).

The exchange between surface water and groundwater can lead to changes in water quality. In areas where heavy extraction occurs, infiltration from surface water bodies is a critical component of recharge to groundwater (Maloszewski et al., 1984). Several of the world's greatest alluvial aquifers, including those along the Nile, the Tigris and Euphrates, and the Indus Rivers, are recharged by infiltration from rivers (Clark and Fritz, 1997). This connection between rivers and aquifers is often used by water resource engineers for understanding or predicting contamination potential and sustainable supply of water (Clark and Fritz, 1997). Precipitation generally exhibits distinct seasonal patterns in $\delta^{18}\text{O}$ and $\delta^2\text{H}$, which can allow for the signal to be approximated by sine waves to evaluate mean transit timing of flow from water bodies (Maloszewski et al., 1984; DeWalle et al., 1997). Similarly, seasonal cycles in ^{18}O are used to measure the fraction of young water in a given system (Kirchner, 2016; Jasechko et al., 2016). Understanding the interactions between these systems is important for the effective management of these systems, particularly if the effects of human-activities has the potential to introduce contaminants (McGuire et al., 2006).

Catchment hydrology describes the quantification of hydrological processes and fluxes for a given watershed; often, the attempts to quantify the numerous parameters that are necessary to characterize the dynamic responses of watersheds are simplistic (Troch et al., 2013; Jasechko et al., 2016). The relationship between river water and groundwater is defined by the recharge,

storage, and discharge characteristics of the watershed; these characteristics are often reflected by the behavior of a system as it responds to precipitation events (Clark and Fritz, 1997). Water isotope studies are thus critical for providing an observational technique for establishing connections between water distribution systems and their respective environmental sources—useful for understanding hydrologic processes influencing the water supply system (McGuire et al., 2006).

The Great Flats Aquifer is a coarse sand and gravel aquifer, deposited approximately 10,000 years ago from the retreat of continental glaciers (Simpson, 1952; Barlow and Leake, 2012). Five communities obtain municipal water from the Great Flats Aquifer, which lies beneath the Mohawk drainage basin in Schenectady (Figure 4).

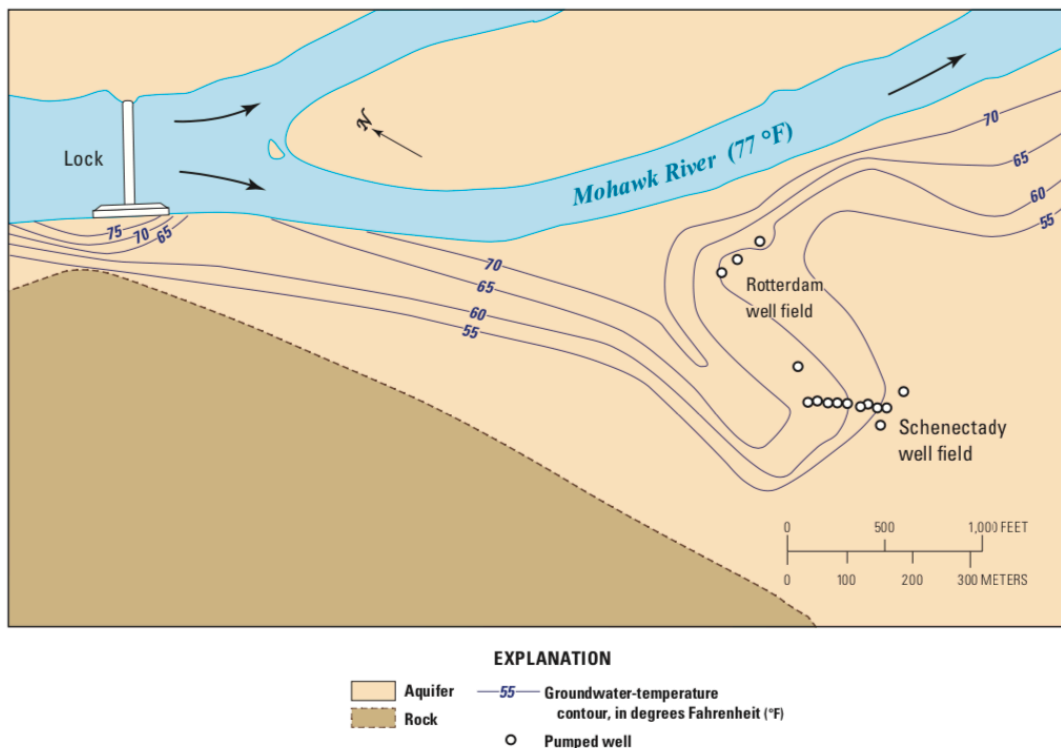


Figure 4. The hydraulic connection existing between surface water and groundwater has been demonstrated by fluctuations in temperature (Barlow and Leake, 2012).

Recharge in the aquifer is controlled mainly by precipitation (directly on land) and seepage from streams; the aquifer principally discharges to the Mohawk River and wells in the adjacent well-field (Waller and Finch, 1982). Schenectady well-fields are sited less than a kilometer from the Mohawk River, making the interaction between surface water and groundwater highly complex and seasonally dependent. This study aims to unravel the surface water and groundwater interactions in the Schenectady region. The collection of groundwater and river water at regular intervals provides the opportunity to understand the transport of water through this system using isotopic compositions (DeWalle et al., 1997). This research is motivated by the need to understand water supply vulnerabilities and to disentangle complex interactions regionally.

2 Characterizing Hydrologic Processes using Groundwater Isotopes

2.1 BACKGROUND

Groundwater recharge occurs as precipitation infiltrates the subsurface and crosses the water table, entering the underlying aquifer. Several factors control the process of groundwater recharge, including the amount of precipitation, evapotranspiration, soil type, vegetation, and climate (Jasechko et al., 2014; Stahl et al., 2020). Precipitation fluxes and vegetation characteristics have been demonstrated as being the most important factors contributing to groundwater recharge (Kim and Jackson, 2012). Because isotopes contain information about the source of water and processes affecting the isotopic composition, stable isotopes can be leveraged to understand the source(s), timing, and efficiency of groundwater recharge. Groundwater is a mixture of its recharge sources; thus, the isotopic signature of groundwater is a weighted average of these sources. Knowledge of the isotopic signatures of the recharge sources provides insight into the relative contributions of these sources. When groundwater is dominantly recharged by precipitation, we can use the seasonal differences in precipitation isotopes to identify the seasonal recharge timing and efficiency.

We examine the seasonality of groundwater recharge using groundwater and precipitation isotopes to determine the importance of each season to recharge. Similarly, we constrain the controls (precipitation amount and/or recharge efficiency) on groundwater recharge. The proportion of recharge describes the contributions from winter and summer precipitation. Recharge efficiency describes the likelihood of the success of recharge, and is independent of the amount of recharge occurring. Determining the seasonal timing of groundwater recharge and environmental factors that influence it is significant, as regional climate and environmental features influence recharge—and changes to climate and subsequent conditions will impact the sustainability of our water resources (Jasechko et al., 2014; Bowen et al., 2019).

2.2 METHODOLOGY

2.2.1 *Data Acquisition*

Groundwater isotope data was obtained from the USGS NWIS and other studies in the scientific literature. The NWIS provides chemical and physical data for wells across the nation, compiled over the past hundred years and over thousands of projects and studies. Data from the NWIS was queried using the `dataRetrieval` package in the R programming language to gather data (Cicco and Hirsch, 2014). The query, which searched the NWIS database for water quality information (isotopes of $\delta^2\text{H}$ and $\delta^{18}\text{O}$) for wells shallower than 45 meters in depth, resulted in nearly 11,000 data points and 7,400 site locations. Only shallow (< 45 m depth) groundwater samples were considered to ensure modern precipitation would reflect groundwater recharge reasonably well (Lindsey et al., 2019). Studies suggest groundwater of depths less than 45 meters are typically aged Holocene or younger, and thus reflect water that has been recently recharged (McMahon et al., 2011; Lindsey et al., 2019). Smaller datasets for areas in the United States with limited water quality information (including Kansas, Colorado, West Virginia, and South Dakota) were gathered by exploring studies in the scientific literature (Clark et al., 1998; Chambers et al., 2015; Iles and Rich, 2017).

Groundwater sites and data acquired from these studies were reviewed using the Environmental Protection Agency (EPA) water quality database¹ to determine the source of water (ensuring groundwater), depth of the well, and precise location (latitude and longitude). Sample dates range from 1976 to 2019. Given the relative scarcity of the data, we determined it is not reasonable to exclude points based on the timing of sampling, as the isotopic variability of groundwater over several decades is minimal. Samples containing isotope values (both $\delta^2\text{H}$ and

¹ <https://www.epa.gov/waterdata/water-quality-data-wqx>

$\delta^{18}\text{O}$), well depth, and spatial coordinates were retained in the dataset, which contained 10,467 samples at 7,266 unique locations (Figure 5) after data cleaning and handling.

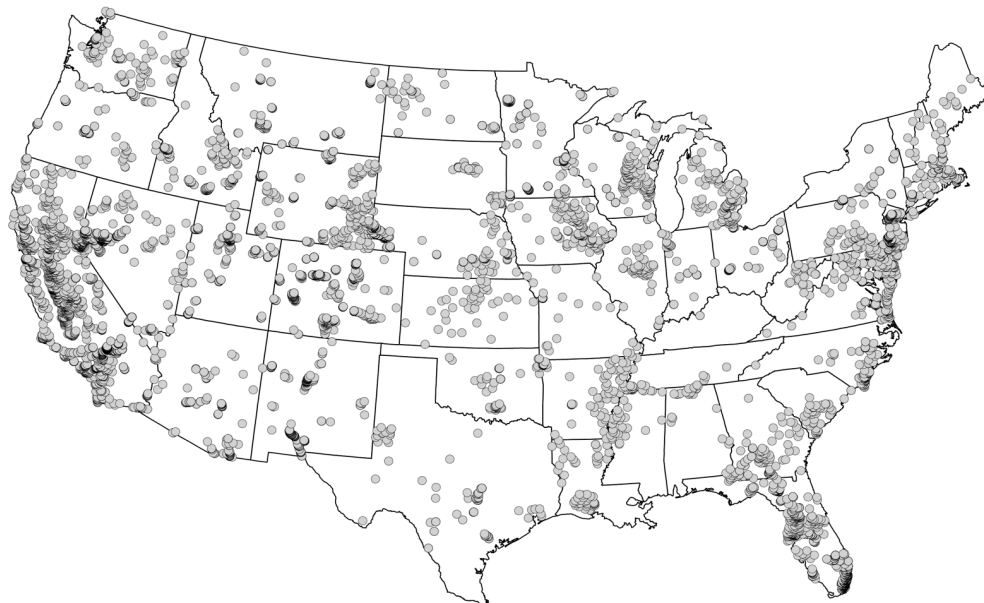


Figure 5. Map showing the locations of the sample sites for the United States ($n = 7,267$).

In addition to the isotope data, supplementary environmental data, including air temperature, annual and monthly precipitation amounts (PRISM Climate Group, 2012), and isotopes of precipitation (Bowen et al., 2005; 2019), were appended to the dataset to understand other factors affecting isotope variability. Mean annual temperature and precipitation data were acquired from the PRISM 30-year normal dataset (PRISM Climate Group, 2012).

2.2.2 Calculating Recharge Proportions and Efficiency

This approach follows the methodology of Jasechko et al. (2014) for calculating the recharge proportions and efficiencies. The year is divided into two seasons, winter and summer, where winter is considered to be October to March and summer is considered to be April to September. We determine the proportion of seasonal contributions from winter and summer precipitation by comparing the isotopic composition of groundwater samples to their respective winter and summer precipitation end-members (Figure 6).

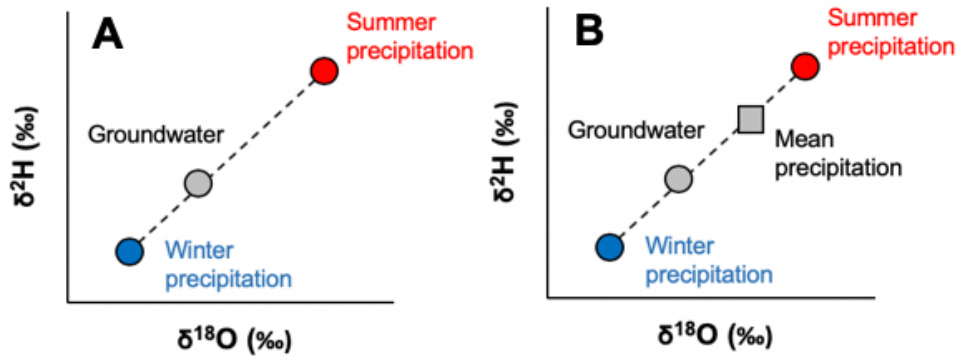


Figure 6. Derivation of the seasonality of groundwater recharge ratio by comparing groundwater isotope values to seasonal precipitation end-members and annual precipitation (modified Jasechko et al., 2014). A) shows the comparison of groundwater isotopes to the precipitation end-members, which determines the proportion of recharge occurring in the summer and winter. B) shows the comparison of groundwater isotopes and precipitation isotope end-members to the weighted annual precipitation isotope value, which determines which season is more efficient at generating recharge. In this hypothetical scenario, mean annual precipitation falls closer to summer precipitation, indicating there is more precipitation in the summer. The groundwater value is closer to winter precipitation, indicating although the major of precipitation falls in the summer, the majority of recharge occurs in the winter.

Seasonal end-members were calculated using the PRISM climate datasets for monthly precipitation and the isotopes of precipitation from Bowen et al. (2005).

$$\delta_{P(\text{Summer})} = \sum_{i=1}^n \frac{P_i}{P_{\text{total (Summer)}}} \times \delta_i$$

$$\delta_{P(\text{Winter})} = \sum_{i=1}^n \frac{P_i}{P_{\text{total (Winter)}}} \times \delta_i$$

where $\delta_{P(\text{Summer})}$ and $\delta_{P(\text{Winter})}$ are the isotopic end-members for winter and summer precipitation, P_i is the precipitation amount (PRISM Climate Group, 2012), P_{total} is the total amount of precipitation in the respective season, and δ_i is the isotopic composition (Bowen et al., 2005).

The seasonal recharge proportions describe the proportion of recharge occurring in the winter and summer. Recharge contributions for winter and summer seasons were calculated using the following linear mixing model:

$$\frac{R_{\text{Winter}}}{R_{\text{Annual}}} = \frac{\delta_{\text{Groundwater}} - \delta_{P(\text{Summer})}}{\delta_{P(\text{Winter})} - \delta_{P(\text{Summer})}}$$

$$\frac{R_{\text{Summer}}}{R_{\text{Annual}}} = 1 - \frac{R_{\text{Winter}}}{R_{\text{Annual}}}$$

where R_{Winter} , R_{Summer} , R_{Annual} represent the recharge fluxes for the winter season, summer season, and annually, $\delta_{\text{Groundwater}}$ represents the isotopic composition of groundwater, and $\delta_{P(\text{Summer})}$ and $\delta_{P(\text{Winter})}$ are the isotopic compositions of summer and winter precipitation (amount-weighted). The resulting ratios allow for the comparison of the proportion of recharge occurring during winter and summer seasons. We categorize the recharge dominance based on where the groundwater samples fall on the mixing line compared to seasonal precipitation end-members. Samples are characterized as follows: winter dominant if $\geq 80\%$ of annual recharge occurred in the winter season, slightly winter dominant if between 60-80% of annual recharge occurred in the winter, summer dominant if $\geq 80\%$ of annual recharge occurred in the summer season, or slightly summer dominant if between 60-80% of annual recharge occurred in the summer season. A sample was determined to have no dominant recharge season if between 40-60% of annual recharge occurred in either season.

The seasonal recharge efficiency ratio describes which season is most effective at generating recharge by comparing the relative proportion of recharge to the precipitation ratio between seasons. Recharge efficiency is calculated by comparing the isotopic compositions of seasonal end members, weighted average precipitation, and groundwater:

$$\frac{(R/P)_{\text{Winter}}}{(R/P)_{\text{Summer}}} = \frac{(\delta_{\text{Groundwater}} - \delta_{\text{P(Summer)}})/(\delta_{\text{P(Annual)}} - \delta_{\text{P(Summer)}})}{(\delta_{\text{Groundwater}} - \delta_{\text{P(Winter)}})/(\delta_{\text{P(Annual)}} - \delta_{\text{P(Winter)}})}$$

where $(R/P)_{\text{Winter}}/(R/P)_{\text{Summer}}$ represents the proportion of precipitation generating winter recharge relative to the proportion of precipitation generating summer recharge, $\delta_{\text{Groundwater}}$ represents the isotopic composition of groundwater, and $\delta_{\text{P(Summer)}}$, $\delta_{\text{P(Winter)}}$, $\delta_{\text{P(Annual)}}$ are the isotopic compositions of precipitation in the summer, winter, and annually.

Seasonal recharge proportions and efficiency were calculated for sites that (1) fell within the seasonal precipitation isotope end-members, (2) were not impacted by evaporation, and (3) exhibited a clear seasonal signal in precipitation isotopes. To account for samples impacted by evaporation, we set a d-excess threshold such that samples with d-excesses < 0 were excluded from these calculations (Jasechko et al., 2014). Samples that did not exhibit significant seasonal variation (difference between amount-weighted summer and winter precipitation $\delta^2\text{H} < 7.5\text{‰}$) were also excluded. We calculated the seasonal recharge proportions and efficiencies for nearly half (5,147 of 10,467) of our samples. For sites demonstrating a dominant season responsible for generating recharge, we identified the factor responsible for the result (Figure 5). Precipitation amount was considered the factor controlling seasonal dominance if precipitation in the dominant recharge season accounted for $> 60\%$ of annual precipitation. Efficiency was considered the factor controlling seasonal dominance if the dominant season was at least 1.5 times more efficient than the other season.

2.3 RESULTS AND DISCUSSION

2.3.1 Regional Patterns in Groundwater Isotopes

The range of stable isotope ratios for groundwater $\delta^2\text{H}$ values is -162.0‰ to 20.51‰ , while the range of stable isotope ratios for $\delta^{18}\text{O}$ is -20.84‰ to 10.00‰ . The average values of $\delta^2\text{H}$ and $\delta^{18}\text{O}$ are -65.20‰ and -8.96‰ , respectively. Most of the groundwater data across the U.S. fall near the Global Meteoric Water Line ($\delta^2\text{H} = 8 \cdot \delta^{18}\text{O} + 10$; Figure 7).

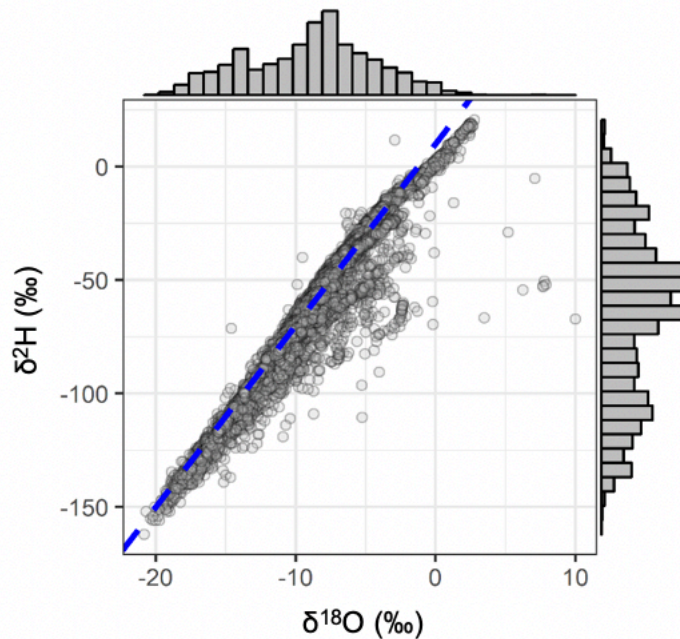


Figure 7. Plot of all groundwater samples and isotopic values ($n = 10,470$), with the global meteoric water line for reference. Distributions of $\delta^2\text{H}$ and $\delta^{18}\text{O}$ values are shown in the marginal histograms.

Some samples fall below the GMWL, indicating evaporative effects. Deuterium excess values were calculated and range from -147.20‰ to 45.67‰ , with a median (average) value of 7.58‰ (6.46‰). Groundwater isotope ratios generally follow a spatial pattern, with the lowest $\delta^2\text{H}$ and $\delta^{18}\text{O}$ values observed along the Rocky Mountains ($<150\text{‰}$ and $<20\text{‰}$) and the highest values observed in states along the Gulf Coast (approximately 0‰). Groundwater isotope values generally follow the signals of isotopes of precipitation, consistent with decreasing values

moving from low-latitude, low-elevation coastal regions into high-latitude, high-elevation, and inland regions.

Environmental parameters have been demonstrated to control groundwater isotopic values. Following the methodology of Kendall and Coplen (2001), we grouped groundwater samples by eastern sites (longitude $< 97^{\circ}\text{W}$; $n = 2,989$) and western sites (longitude $> 97^{\circ}\text{W}$; $n = 4,436$) to understand the relationship between $\delta^{18}\text{O}$ and environmental parameters, including elevation, temperature, latitude, and precipitation (Figure 8).

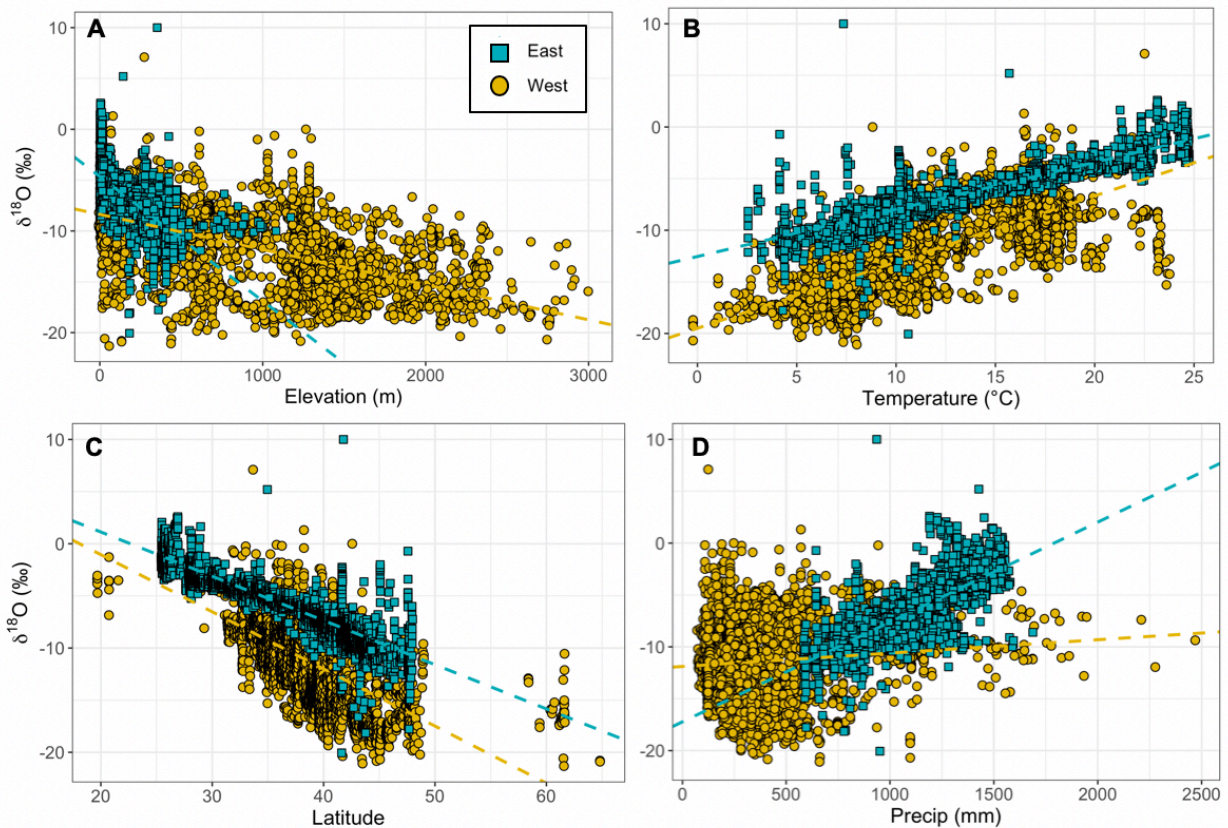


Figure 8. Sites are divided by longitude, where eastern sites are $< 97^{\circ}\text{W}$ and western sites are $> 97^{\circ}\text{W}$. Relationship between groundwater $\delta^{18}\text{O}$ and (a) elevation (eastern sites $r^2 = 0.43$, western sites $r^2 = 0.38$), (b) temperature (eastern sites $r^2 = 0.76$, western sites $r^2 = 0.56$), (c) latitude (eastern sites $r^2 = 0.74$, western sites $r^2 = 0.40$), and (d) mean annual precipitation amount (eastern sites $r^2 = 0.56$, western sites $r^2 = 0.008$). Eastern sites are determined by longitude $< 97^{\circ}\text{W}$ and western sites are $> 97^{\circ}\text{W}$.

There is a relatively weak correlation between eastern ($r^2 = 0.43$) and western ($r^2 = 0.38$) sites and elevation (Figure 8a). Elevation ranges are more clustered in eastern sites, but scattered across the western sites. It is possible the weak correlation is associated with seasonal differences in topographical effects. For eastern sites, there is a strong correlation between $\delta^{18}\text{O}$ and temperature ($r^2 = 0.76$; (Figure 8b). This result is similar to what is typically observed for precipitation and river water samples (Kendall and Coplen, 2001). Western sites display a greater scatter between $\delta^{18}\text{O}$ and temperature ($r^2 = 0.56$), perhaps due to the larger seasonal ranges in temperature due to more irregular topography compared to eastern sites. A strong correlation between $\delta^{18}\text{O}$ and latitude in the east ($r^2 = 0.56$; Figure 8c). This relationship is likely a result of the strong correlation between $\delta^{18}\text{O}$ and temperature in this region. Western sites are consistent with a weaker correlation related to latitude ($r^2 = 0.40$), which could also be attributed to the moderate correlation between this region and temperature (given the greater seasonal variability). Precipitation amount is moderately correlated with isotopic values in the east ($r^2 = 0.56$), and has no linear correlation with isotopic values in the west ($r^2 = 0.008$; Figure 8d). The scatter in the west could be due to various climatic effects in the west, such as greater seasonality with respect to the amount or source of precipitation. Because the climatic data used were the average values recorded at each location, the correlation between isotopic values and these parameters are quite good despite the heterogeneity among locations.

Groundwater data was grouped by state to calculate the slopes and intercepts of the groundwater lines (GWLs) using the Theil-Sen fit and least squares fit (Table 1).

Table 1. Slopes and intercepts of the GWLs for each state.

State	Theil-Sen		Least Squares		Samples
	Slope	Intercept	Slope	Intercept	
AK	6.76	-17.47	6.78	-17.85	41
AL	6.2	3.57	6.73	6.48	26
AR	6.12	3.01	4.68	-5.39	78
AZ	7.6	0.89	6.7	-6.11	130
CA	7.73	3.42	6.88	-5.32	1724
CO	6.87	-9.51	6.93	-8.92	374
CT	6.23	0.65	6.66	3.84	43
DE	5.33	-3.31	4.56	-8.58	35
FL	5.6	2.26	5.57	2	536
GA	6.24	4.56	6.1	4.25	83
HI	5.37	3.88	7.48	9.41	15
IA	7.91	11.28	7.79	10.31	126
ID	6.84	-14.3	7.22	-7.9	150
IL	7.66	10.66	7.89	11.94	64
IN	7.5	9.66	8.18	14.22	34
KS	6.89	2.21	6.8	0.89	40
KY	1	-34.47	1	-34.47	2
LA	6.22	5.12	5.6	2.37	57
MA	5.25	-7.05	5.48	-6.16	235
MD	7.21	8.95	7.19	8.75	63
ME	7.61	9.96	6.71	0.72	15
MI	7.23	5.35	7.45	7.49	138
MN	7.25	2.44	5.76	-14.58	256
MO	9.54	21.16	9.69	22.12	36
MS	5	-2.43	0.72	-23.8	30
MT	5.2	-43.52	5.63	-38.19	127
NC	6.2	4.53	5.97	3.56	127
ND	8.62	14.45	8.42	13.2	42
NE	8.64	13.17	8.75	13.54	252
NH	8.72	20.34	8.81	21.33	11
NJ	6.55	3.92	5.85	-1.86	175
NM	6.7	-9.53	6.42	-12.58	187
NV	6.19	-21.7	4.82	-41.53	533
NY	7.49	8.46	7.77	11.03	43
OH	7.7	10.36	7.66	10.74	91
OK	7.31	8.71	6.66	4.44	55

OR	7.51	-1.01	8.12	6.34	97
PA	9.03	23.56	1.17	-48.2	79
RI	NA	NA	NA	NA	NA
SC	6.64	5.63	6.1	3.39	62
SD	7.92	9.27	7.82	7.96	65
TN	6.38	4.26	6.19	3.34	27
TX	9.63	17.5	8.68	11.52	65
UT	5.88	-27.65	5.42	-34.2	196
VA	7.6	11.57	7.63	11.78	142
VT	7.87	12.76	8.04	14.33	4
WA	8.48	13.84	8.54	14.03	135
WI	7.98	12.14	6.96	1.93	180
WV	7.08	7.74	7.22	7.4	31
WY	6.43	-21.74	6.36	-23.23	265

*Note that RI slopes and intercepts could not be calculated due to lack of data in this state.

Linear regression models are typically used for determining the slopes and intercepts for compared $\delta^2\text{H}$ and $\delta^{18}\text{O}$ values (e.g. LMWL). We additionally calculate the slopes and intercepts using the Theil-Sen method, as this method follows simple linear regression but can be more robust against outliers. By state, the slopes ranged from 1.00 to 9.63, with an average slope of 6.98. The lowest slope was observed in Kentucky, although the lack of sufficient data in this state may contribute to likely error in this estimate. The highest slope (9.63) was observed in Texas, a much higher value than the river water line (RWL) slope of 7.5 reported by Kendall and Coplen (2001).

Groundwater data is grouped by the regional USGS hydrologic unit code to calculate the slopes and intercepts of the GWLs for each watershed (Figure 9).

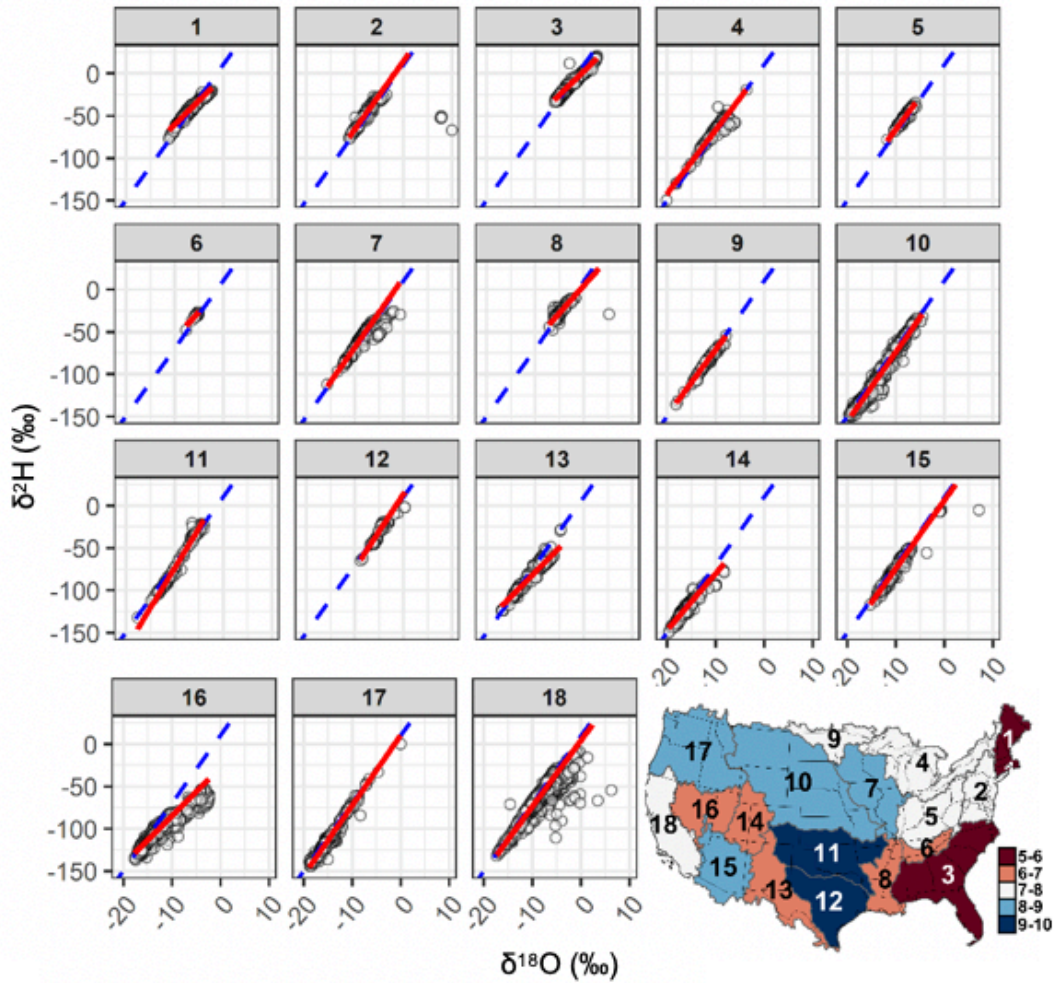


Figure 9. Plot of $\delta^2\text{H}$ and $\delta^{18}\text{O}$ values by HUC code, with the GMWL (dashed blue) and the LMWL (red line) determined by the Theil-Sen fit.

Results for the Theil-Sen fits and the least square fits for groundwater data by HUC are displayed in Table 2.

Table 2. Slope and intercepts of the GWLs for each HUC code.

HUC-02	Theil-Sen		Least Squares		Samples
	Slope	Intercept	Slope	Intercept	
1	5.4	-5.94	5.84	-4.01	309
2	7.66	11.96	5.42	-5.4	509
3	5.74	2.61	5.67	2.15	846

4	7.53	8.19	6.98	2.08	319
5	7.77	11.55	7.49	9.37	133
6	6.2	4.17	7.52	10.84	23
7	8.29	14.34	6.17	-5.58	384
8	6.67	5.6	3.71	-8.48	144
9	7.67	5.19	7.46	1.74	84
10	8.09	5.73	8.33	9.37	826
11	9.1	19.14	9.12	18.3	179
12	9.5	17.35	8.49	10.77	71
13	6.26	-15.29	6.37	-13.79	229
14	6.6	-14.97	6.49	-17.36	193
15	8.1	6.73	7.09	-4.24	216
16	6.07	-23.5	4.97	-39.9	678
17	8.22	8.96	8.14	7.79	407
18	7.76	3.87	6.91	-5.16	1716

There is not a strong spatial correlation observed for calculated GWLs of the HUCs. Slopes ranged in values from 5.4 to 9.5, with an average slope of 7.37. The lowest slope was observed in HUC-01 (basins of New England), while the highest slope was observed in HUC-12 (basins of Southeastern Texas). Slopes between 7 and 8, which are consistent with the GMWL, are observed for California, the Great Lakes region, and the central eastern basins (HUCs 02, 04, 05, 09, 10, 17, and 18). We compare the low slope calculated in HUC-01 to the slope of the RWL reported by Kendall and Coplen (2001). Kendall and Coplen (2001) report a slope of 7.1 for HUC-01, despite slope estimates between 5 and 6 for Connecticut and Massachusetts. We attribute our slope value to the vast amount of groundwater samples for HUC-01 located in these states. Additionally, it is possible this low slope suggests HUC-01 is influenced by effects of evaporation in groundwater samples—particularly in Cape Cod, Massachusetts, where significant proportions of groundwater are recharged by ponds (Masterson, 2004; Walter et al., 2004). Thus, climate and coastal processes may influence regional groundwater lines in watersheds.

2.3.2 Seasonal Recharge Efficiencies

Seasonal recharge efficiencies were calculated for 5,147 samples and demonstrate coherent spatial patterns (Figure 10).

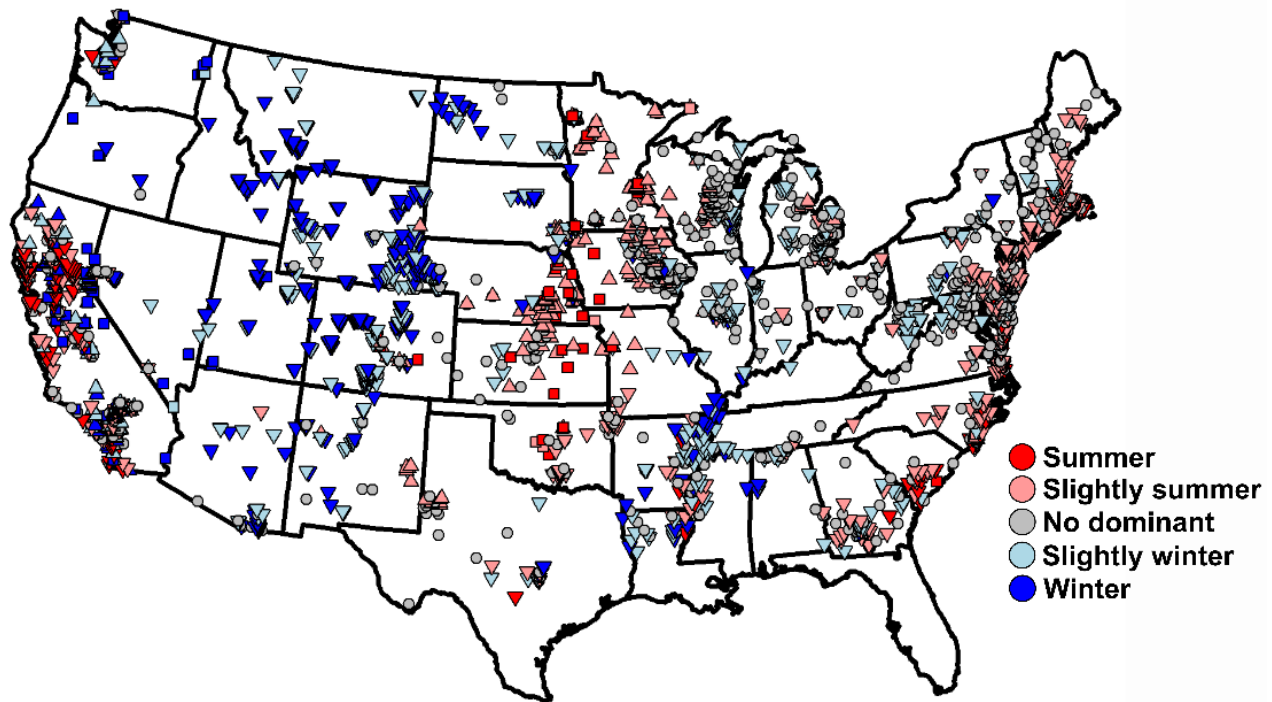


Figure 10. Calculated recharge proportions for all of the sampling locations that allowed for calculations. Samples are colored by the seasonal dominance. The shape denotes the control on seasonal dominance; an upward pointing triangle indicates precipitation amount controls the seasonal dominance, while a downward pointing triangle indicates the seasonal dominance is efficiency controlled; a square indicates both contribute to the dominant season.

With some notable exceptions, the majority of groundwater samples have calculated seasonal efficiency ratios greater than 1, suggesting a winter bias in recharge. This winter bias is likely the result of lower potential for ET during the winter due to colder temperatures and less vegetation. Along the eastern U.S., winter and summer contribute similar amounts of recharge (no dominant season). On the east coast, a slight summer bias is observed. This bias in recharge is perhaps a result of the shallow water tables along the coast (Fan et al., 2013), which prevents further recharge during the winter. Winter recharge becomes more efficient relative to summer

recharge (by a magnitude of 1.5-3 times more efficient) moving 50 km from the eastern coast. This winter bias in recharge is consistent with decreasing potential for ET during the winter due to cooler temperatures and dormant vegetation.

Summer recharge is more efficient relative to winter recharge in the central U.S., notably Texas, Oklahoma, Eastern Kansas, and Eastern Nebraska (Figure 11).

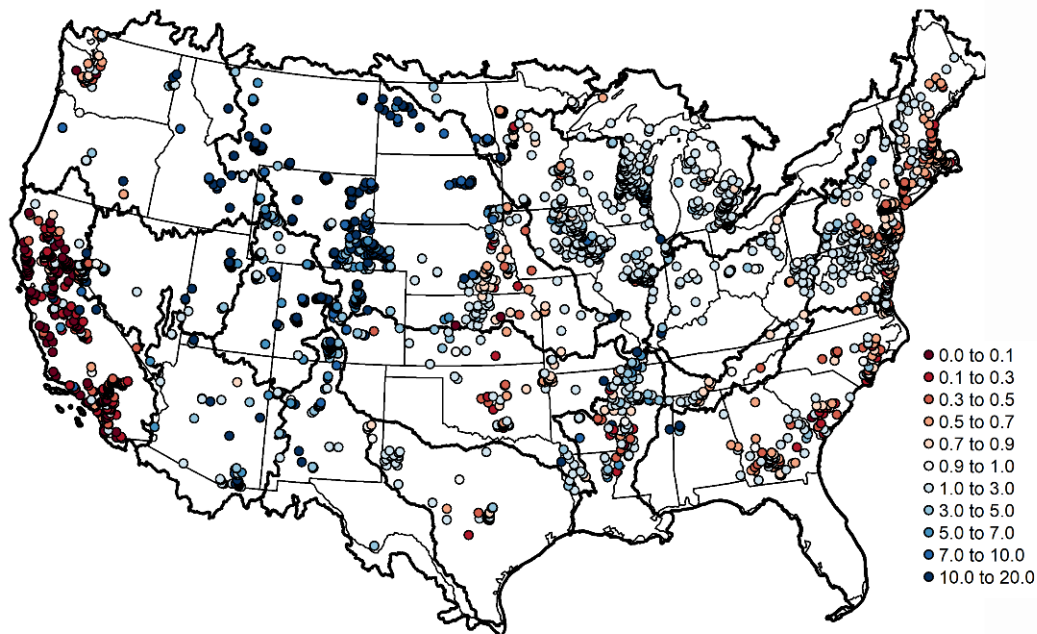


Figure 11. Map of calculated recharge efficiency ratios (winter/summer) at groundwater sample locations.

Unique meteorological conditions in this region potentially result in the summer bias in recharge efficiency, as this area coincides with convective storms during the summer that occur at night. The majority of summer precipitation occurs nocturnally, when ET and temperatures are lower and likely allows for more groundwater recharge (Balling, 1985). In the western interior (WY, CO, NM, ID, UT, AZ, and NV), winter recharge is more efficient than summer recharge (by a magnitude of at least 5; Figure 6). This result indicates per unit of precipitation, winter generates more recharge than the summer. We attribute the strong bias towards winter recharge to be a

result of lower ET in winter relative to summer, as the vapor pressure deficit is high in the summer—driving high rates of ET (PRISM, 2012).

2.3.3 *Seasonal Recharge Proportions*

Seasonal recharge proportions were calculated for 5,147 samples and demonstrate similar coherent spatial patterns (Figure 10). The efficiency of recharge for a given season (e.g., the proportion of precipitation that actually recharges) and the amount of precipitation (e.g., the supply of water) determine the resulting seasonal contributions to annual recharge (Figure 11). Groundwater recharge does not display a seasonal dominance for much of the U.S. east of the Mississippi River. A slight summer dominance in recharge proportion is observed along the east coast, which we attribute to the summer bias in efficiency identified in these sites. The slight winter dominance in the Appalachian Mountain area (VA, WV, and PA) and northern section of Mississippi is also attributed to a bias in efficiency; here, winter dominance is a result of the greater efficiency of winter recharge relative to summer.

In the central U.S. (immediately west of Mississippi), groundwater recharge is slightly summer to summer dominant, perhaps due to the seasonal differences in the amount of precipitation as the majority of precipitation (>60%) falls during the summer. A strong summer dominance is observed in Oklahoma, Eastern Kansas, and Eastern Nebraska; these sites are consistent with the majority of precipitation falling in the summer and more efficient summer recharge. Throughout the Northern Great Plains (ND, SD, MT) and Western interior (WY, CO, NM, ID, UT, AZ, NV), a consistent slightly winter to winter dominance is observed. This observation is the result of the strong winter bias in recharge efficiency—despite lower amounts of precipitation in some of the areas, winter is disproportionately effective at generating recharge.

2.3.4 West Coast Processes

Groundwater isotopes in Coastal California are closer to isotope values consistent with summer precipitation, and in some cases heavier than summer precipitation values (Figure 10). Groundwater isotopes that are heavier than mean annual precipitation isotopes, and in many cases heavier than summer precipitation. This observation is suggestive of summer dominant recharge. However, little precipitation (< 10% of the annual precipitation amount) occurs in the summer in California, suggesting the result of summer recharge is consistent with very efficient summer recharge or very inefficient winter recharge—contradicting the common understanding of the process of groundwater recharge. We identified sites consistent with summer recharge are areas frequently inundated with fog in the summer months (Figure 12).

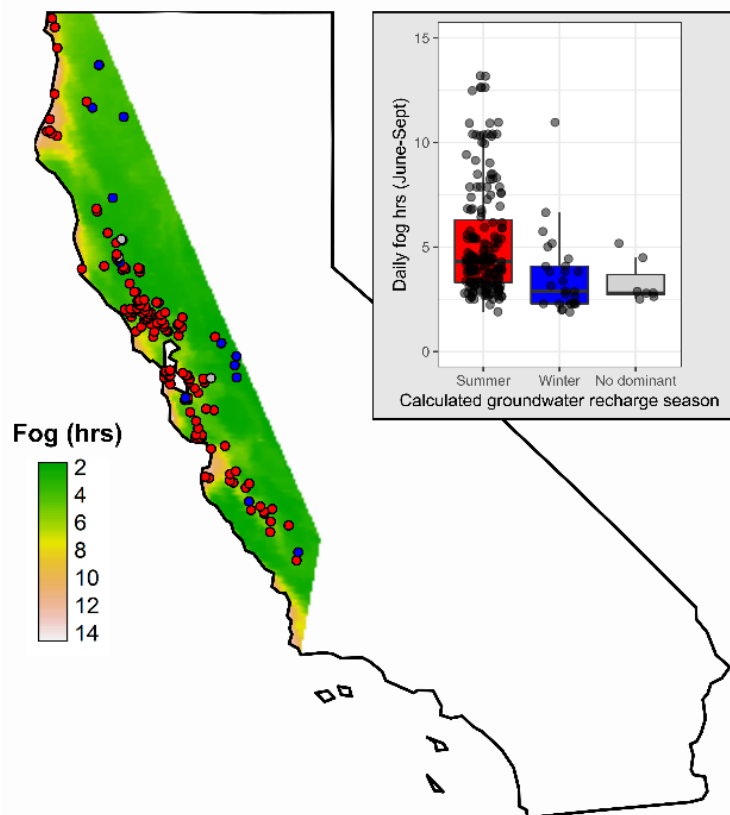


Figure 12. Dominant recharge season for coastal California groundwater samples compared to daily hours of summer (June to September) fog cover. The dominant recharge season for

groundwater samples are colored by dominant recharge season (summer = red; winter = blue). The boxplot shows the distribution of fog cover for samples based on dominant recharge season.

Fog, which occurs in the summer from June to September in California, is isotopically the heaviest atmospheric water, with isotope values enriched relative to annual and summer precipitation values (Ingraham and Matthews, 1990; 1995). Our results indicate areas demonstrating a summer dominance in recharge—driven by fog as opposed to summer precipitation in other sites—had significantly higher hours of daily fog cover than other samples. Thus, fog can contribute to groundwater recharge in coastal areas. Infiltration and ultimately recharge from fog can occur as a result of fog moving in from the coast, coalescing on vegetation, and dripping into the ground. This process has been minimally studied relative to its importance to groundwater, while several studies have demonstrated the importance of fog drip to plants on a more local scale (Dawson, 1998; Corbin et al., 2005).

Although fog contribution to groundwater along coastal California has been only minimally studied, evidence for fog contributions to groundwater in other regions has been demonstrated. Fog drop in excess of rainfall has been reported near Cape Town, South Africa—an environment similar to that of coastal California (Nagel, 1956). The potential for recharge from fog water is further demonstrated by the observation reported by Marloth (1905), in which fog events were determined to increase river stages and cause pools of water on the upper plateau of Table Mountain. Other areas in which fog has been demonstrated to be a contributor to groundwater include Maui, Hawaii (Scholl et al., 2002), and aquifer systems in the coastal forests of Oman (Clark et al., 1987; Strauch et al., 2014). Because these areas are consistent with coastal and forested areas consistent with fog cover, there is the potential for fog contributions to

groundwater in other areas in the U.S. Our results suggest further study on the role of fog inducing groundwater recharge is necessitated.

2.4 CONCLUSIONS

Groundwater contains information about the timing and efficiency of recharge. We have applied an isotopic analysis of groundwater and precipitation data to understand the physical hydrology and seasonal controls on recharge for thousands of sites across the United States. We identify coherent spatial patterns in groundwater isotopes and recharge timing, and correlate isotopic values to environmental parameters. Additionally, we observe notable features in coastal California (e.g. fog contributing to groundwater recharge) and the central U.S. (e.g. intense nocturnal precipitation events). Characterizing groundwater recharge across the United States is critical for ensuring the sustainability of future water resources, particularly as changes to climate may result in differences in seasonal effects on groundwater recharge. Thus, it is essential to understand recharge processes across the United States.

3 Development of a National Isoscape

3.1 BACKGROUND

Isoscapes, which map the distribution of a given parameter, are not only useful for understanding hydrologic processes—having applications across a wide variety of disciplines, including ecology, environmental forensics, and climatology (Bowen and Good, 2015; West et al., 2009). In addition, isotopes in groundwater contain information about when the water recharges, which is useful for understanding potential perturbations; however, such processes are difficult to understand given the lack of measurements across all locations. Models or interpolations (isoscapes) have been used to understand the spatial distribution of environmental parameters (Kendall and Coplen, 2001; Bowen and Good, 2015). While these types of maps exist for isotopes in natural waters (e.g. precipitation and rivers), there was not a previously developed cohesive map of groundwater isotopes for the United States (Kendall and Coplen, 2001; Dutton et al., 2005). Thus, many studies in hydrology are limited by the lack of compiled information for groundwater (Bowen and Good, 2015).

There are many geostatistical and mathematical approaches for generating spatial predictions for environmental variables such as isotopes, although most methods are dependent upon the spatial resolution of available data and variables which are dependent on one another. Here, we utilize two different approaches to transform measurements of isotopes in groundwater into predictive surfaces: kriging and random forest modeling. These models provide powerful tools for estimating isotopes of groundwater when there is no such data available, as well as the basis for further hydrologic analysis (Stahl et al., 2020).

The kriging method is a widely used technique in environmental science and monitoring (Zirschky, 1985). Kriging has been used in groundwater quality assessment for understanding the distribution of concentrations of parameters in groundwater, as well as in soil science,

agronomy, and environmental monitoring (Zhang et al., 1996; Al-Mashagbah et al., 2012). Ordinary kriging is a purely spatial correction, based on the assumptions of stationarity and isotropy across the study space (Gimond, 2017). Predictions are developed by modeling spatial dependence between neighboring points, with the spatial weights estimated by a statistical model (the sample variogram) as opposed to a mathematical function used in other interpolation methods (Zirschky, 1985; Gimond, 2017). This method does not take contextual evidence (e.g. environmental parameters) into account, simply interpolating the value based on two points. A sample variogram, which displays the covariance between pairs of points in the sample set, is used to calculate the weights for each point based on the spatial structure of the dataset. The value of the predicted points and the weight of the value is applied to generate the interpolated surface (Zirschky, 1985; Gimond, 2017). The importance of developing a good sample variogram is highlighted by the dependence of the kriging variance (Zirschky, 1985). Using solely the spatial correlation or spatial trends between points is a major limitation compared to other models, including random forest models.

Random forest (RF) models have been increasingly implemented in studies involving complex ecologic and environmental datasets, demonstrating high predictive capacities across marine and terrestrial sciences (Knoll et al., 2019; Ouedraogo et al., 2019). Beisner et al. (2012) used RF modeling to interpolate nitrate and arsenic concentrations in the southwestern United States for assessing areas with the potential to exceed concentrations above the drinking water quality standard. Knoll et al. (2019) demonstrated the use of RF models to map the concentrations of nitrate in groundwater and compared its performance to other approaches. Similarly, the predictive performance of RF models has been analyzed using complex environmental datasets (Fox et al., 2020).

Random forest models, essentially a collection decision trees, create a “forest” with the best prediction based on predictor variables; the method follows the idea that the overall result is improved with an increasing combination of learning models (Knoll et al., 2019; Fox et al., 2020). Predictor variable selection is critical for optimal RF performance, as the model depends on strong features. The model prediction is based on the predictions of all trees in the forest. RF models are composed of a forest built from training data points, and the generalization of new data based on learning from the forest—the testing data set (Ouedraogo et al., 2019). Compared to other methods, such as logistic models and GLMs, RF models are often more robust and accurate as they utilize variance reduction (Knoll et al., 2019). An advantage of RF models is its ability to compute variable importance, which allows for a greater understanding of influential variables—particularly useful for understanding isotopic concentrations (Beisner et al., 2012; Ouedraogo et al., 2019). A significant limitation of decision trees is the problem of overfitting, which can occur if there are not enough trees generated in the forest; the tendency to overfit is reduced by adding trees to the forest (Fox et al., 2020). Our RF models allow for the prediction of isotope composition for $\delta^2\text{H}$ and $\delta^{18}\text{O}$ using important environmental parameters as predictors.

3.2 METHODOLOGY

3.2.1 *Kriging Approach*

All of the data preparation was performed in R (R Core Team, 2018). The average isotope values of $\delta^2\text{H}$ and $\delta^{18}\text{O}$ were calculated for each unique site ($n = 6,418$) in the groundwater isotope dataset, such that each point represented the average value. The *gstat* package in R was used to generate a sample variogram using an exponential model on the data points for $\delta^2\text{H}$ and $\delta^{18}\text{O}$ (Pebesma, 2004). We estimated the sill and range of the variogram to be

700 (distance) and 850 (variance), respectively. The fit of the variogram determined how values of nearby points were weighted by relating latitude and longitude coordinates (Figure 13).

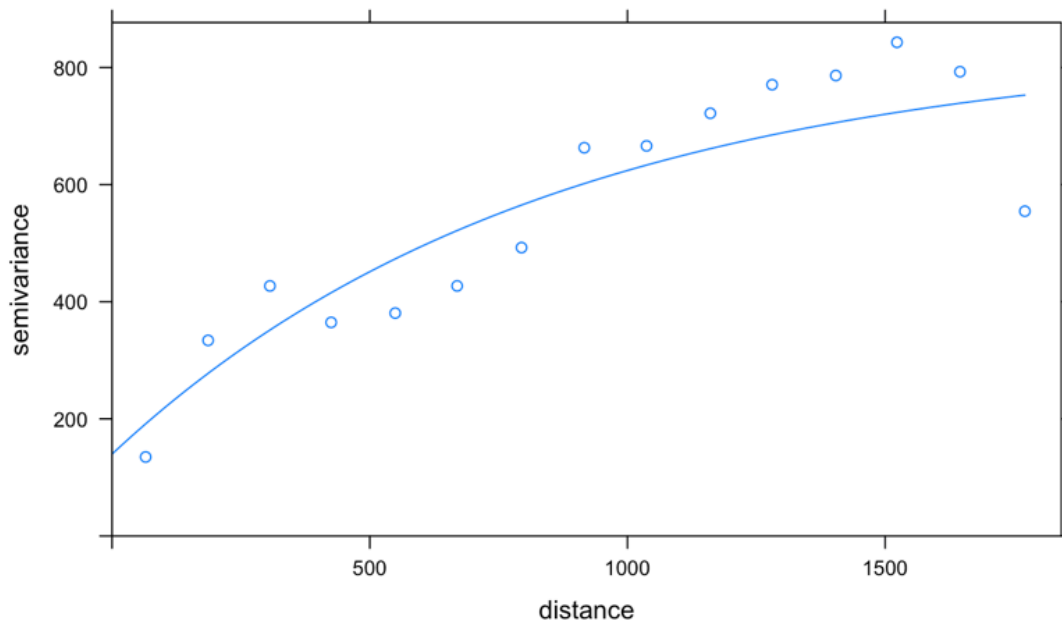


Figure 13. Sample variogram used to calculate how the values of nearby points are weighted for the model fit for the kriging approach; the range and sill are manually calculated.

The raster package in R was then used to create the interpolated surface given by the variogram fit (Hijmans, 2019). The isoscape reflects the interpolated surface created using the kriging method (Figure 14 and 15). Uncertainties in this projection follow the predictions being based on localized factors (Gimond, 2017).

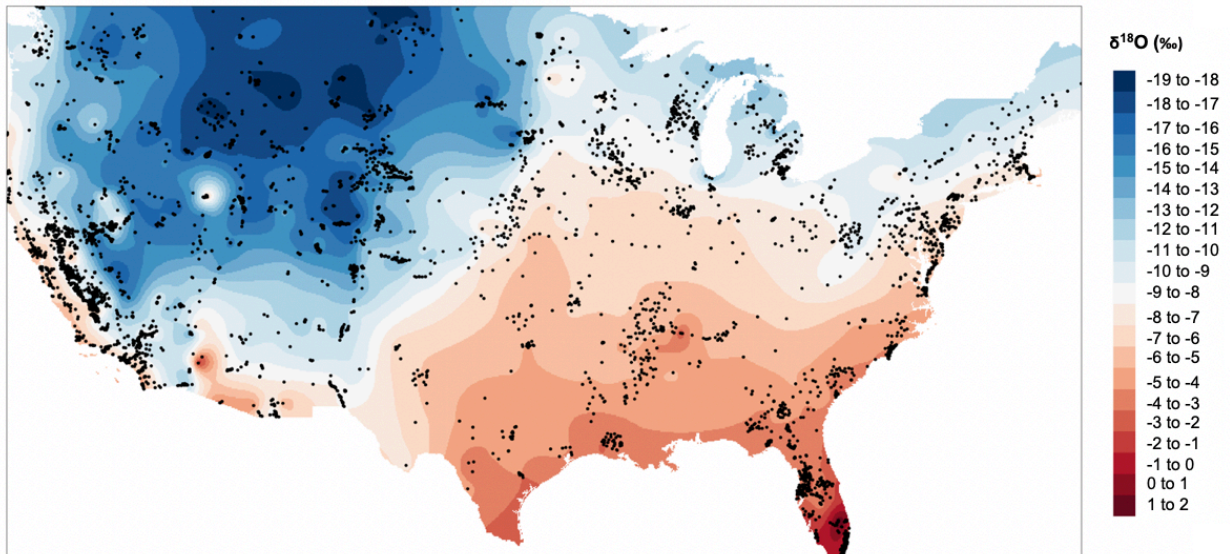


Figure 14. Interpolated isotopic values for $\delta^{18}\text{O}$ using the kriging approach ($n = 6,418$); sample sites are shown as points on the surface.

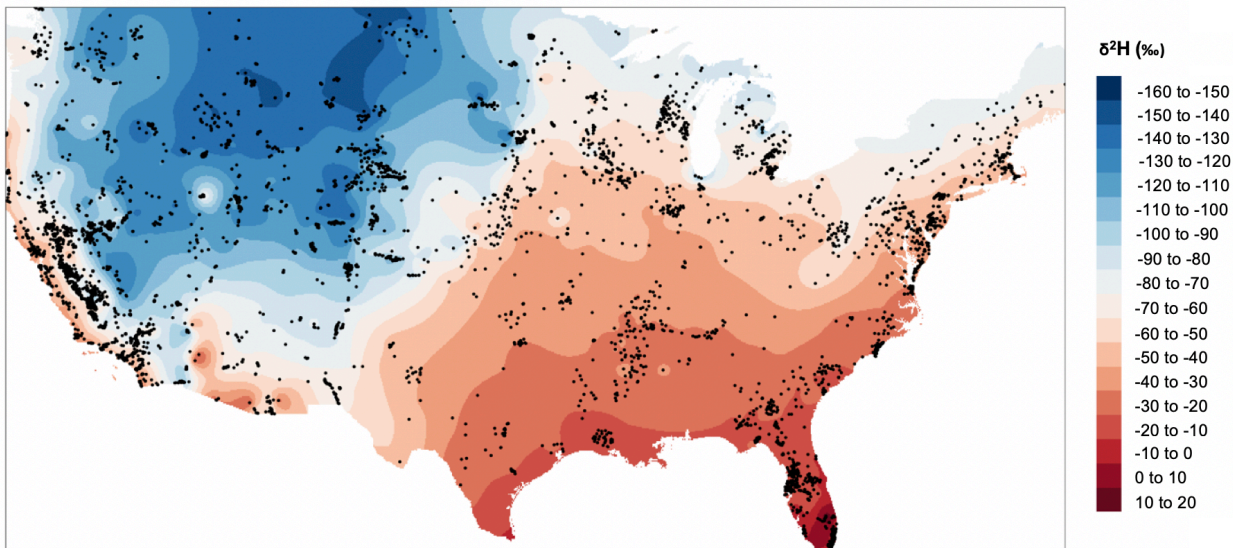


Figure 15. Interpolated isotopic values for $\delta^2\text{H}$ using the kriging approach ($n = 6,418$); sample sites are plotted on the surface.

3.2.2 Random Forest Model

We compiled relevant environmental and geographic data for each unique location in our groundwater isotope dataset; a dataset of approximately 8 key attributes was created. The list of predictive variables, extracted from available raster datasets or included in the NWIS sample metadata, are given in Table 3.

Table 3. List of the environmental parameters evaluated in the random forest model.

Predictor Variable	Data Source	Included in final RF model? (Y/N)
Precipitation isotopes	Bowen 2019 and Bowen et al., 2005	Y
Summer precipitation isotopes	Bowen 2019 and Bowen et al., 2005	Y
Winter precipitation isotopes	Bowen 2019 and Bowen et al., 2005	Y
Precipitation amount (monthly)	PRISM 30-year normals	Y
Elevation	PRISM elevation dataset	Y
Mean annual air temperature	PRISM 30-year normals	Y
Distance to coast	Computed	Y
Latitude	Grid location	Y
Longitude	Grid location	Y
Topsoil (0-30 cm) clay content	Unified North American Soil Map	N
	International Satellite Land-Surface	N
Median topographic slope	Climatology Project, Initiative II	
	Global Reference Evapotranspiration (ET0) Climate Database v2. CGIAR-	N
Annual potential evapotranspiration	CSI	
Seasonal precipitation proportions	PRISM 30-year normals	N
Depth to water table	Fan et al., 2013	N

The environmental parameters considered in the random forest model are related to the isotopic ratios and likely account for much of the variability in the groundwater isotope dataset (Figure 16). Data preparation and spatial transformations were performed in R (R Core Team, 2018).

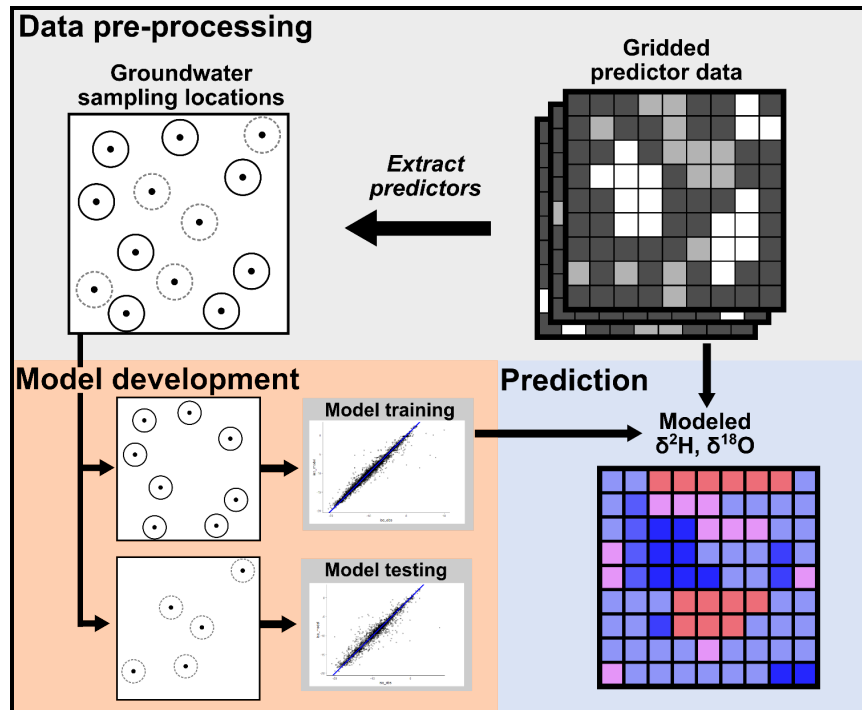


Figure 16. Schematic of the random forest modeling approach. The approach uses environmental parameters along with a training and test set to generate the predicted surface (Stahl et al., 2020).

The samples ($n = 9,880$) were divided into a training (70%) and test set (30%) for the model to understand the relationship between processes influencing isotopic compositions and to avoid overfitting. Using the randomForest package in R to implement the random forest algorithm, we generated approximately 500 trees with each split testing three variables (Liaw and Wiener, 2002). Other environmental parameters (e.g. soil texture, evapotranspiration, and depth to water table) were tested during the model development, but did not improve the model performance and thus were not included in the final model. The parameters with the most predictive power are determined by the importance in the model. The developed model was used to predict groundwater $\delta^2\text{H}$ and $\delta^{18}\text{O}$ values for the United States by applying the RF model to the predictor variables to create a gridded (4 km x 4 km) raster map of the groundwater. The interpolation allows for predicted concentrations where data were previously unavailable. We

estimate the uncertainty of the predicted groundwater isotopes in each grid cell by incorporating the reported uncertainty from isotopes of precipitation (the strongest predictive variable) to compute standard deviations (Stahl et al., 2020).

3.3 RESULTS

3.3.1 *Kriging Approach*

We used a kriging approach to generate an interpolated surface of $\delta^2\text{H}$ and $\delta^{18}\text{O}$ values for groundwater. General patterns of isotopes across the United States are observed using the preliminary isoscape (Figure 14 and 15). A clear spatial trend is recognized by comparing isotopes in the western United States to the eastern United States. Western sites have a greater abundance of lighter isotopes (more negative values), while isotopes of eastern sites have a greater abundance of heavier isotopes (more positive values). Coastal sites follow a similar trend, as these areas are enriched in the heavy isotopes. The similarity of river water isotopes modeled using the same kriging method provides confidence in the resulting isoscape (Kendall and Coplen, 2001). Additionally, we compute a confidence interval map for the kriged surface (Figure 17).

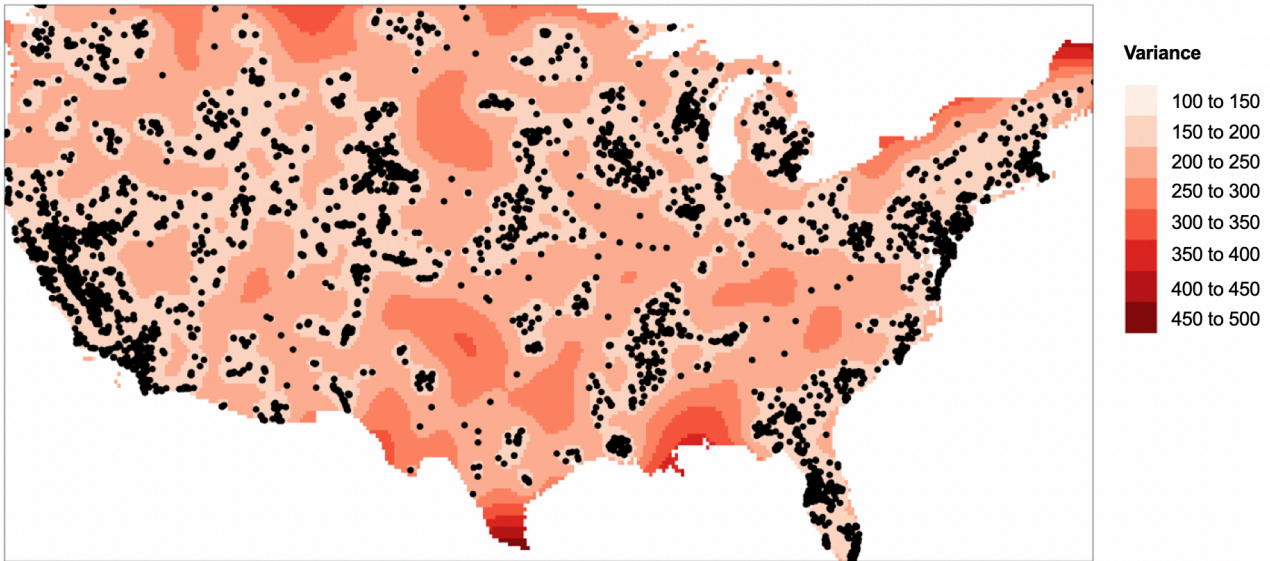


Figure 17. Confidence interval map (95%) for the interpolated $\delta^2\text{H}$ values.

3.3.2 *Random Forest Model*

The random forest (RF) predicts isotopes of $\delta^2\text{H}$ and $\delta^{18}\text{O}$ in groundwater for the conterminous United States using predictor variables. The predictor variables, which were selected based on environmental parameters which are likely to affect the isotopic composition of groundwater, are ranked according to their importance in the model (Wassenaar et al., 2009; West et al., 2014). The most important covariates in our model are amount weighted annual precipitation isotope values, winter and summer amount weighted precipitation isotopes, elevation, and annual precipitation amount (Table 3). Our RF model explains 99% and 98% of the variance for $\delta^2\text{H}$ and $\delta^{18}\text{O}$, respectively, in the training data set, and 97% and 94% of the variance in $\delta^2\text{H}$ and $\delta^{18}\text{O}$ for the test data set; thus, we determine our model performed well, as the predictors accounted for the observed spatial patterns in isotopes of groundwater.

A coherent spatial pattern is observed in isotopes of groundwater across the United States (Figures 18 and 19). The most depleted isotope values for $\delta^{18}\text{O}$ are consistent within the

country's interior and the Rocky Mountains. The Gulf Coast exhibits the highest values of groundwater isotopes and decrease moving north.

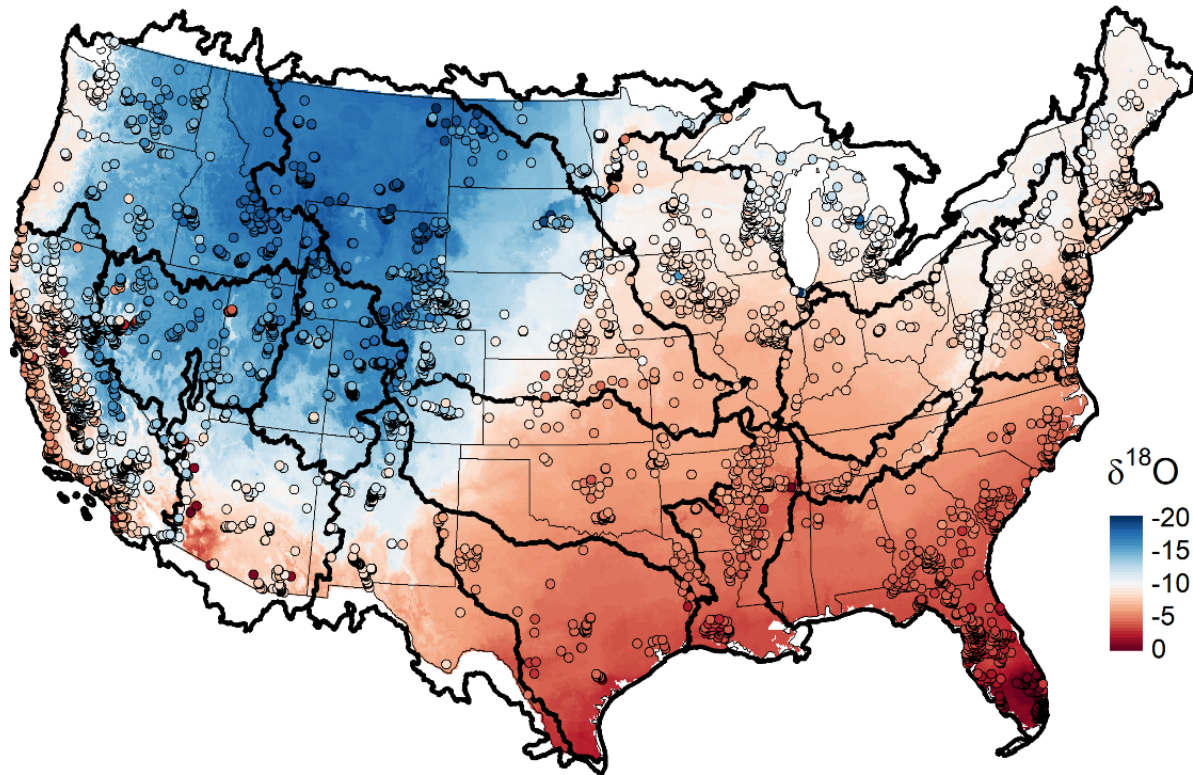


Figure 18. The interpolated surface generated for $\delta^{18}\text{O}$ in groundwater using the Random Forest model (Stahl et al., 2020). Observed values for isotopes are displayed as points. The important predictor variables in this model are annual amount weighted precipitation isotopes, elevation, annual precipitation amount, longitude, and mean annual air temperature.

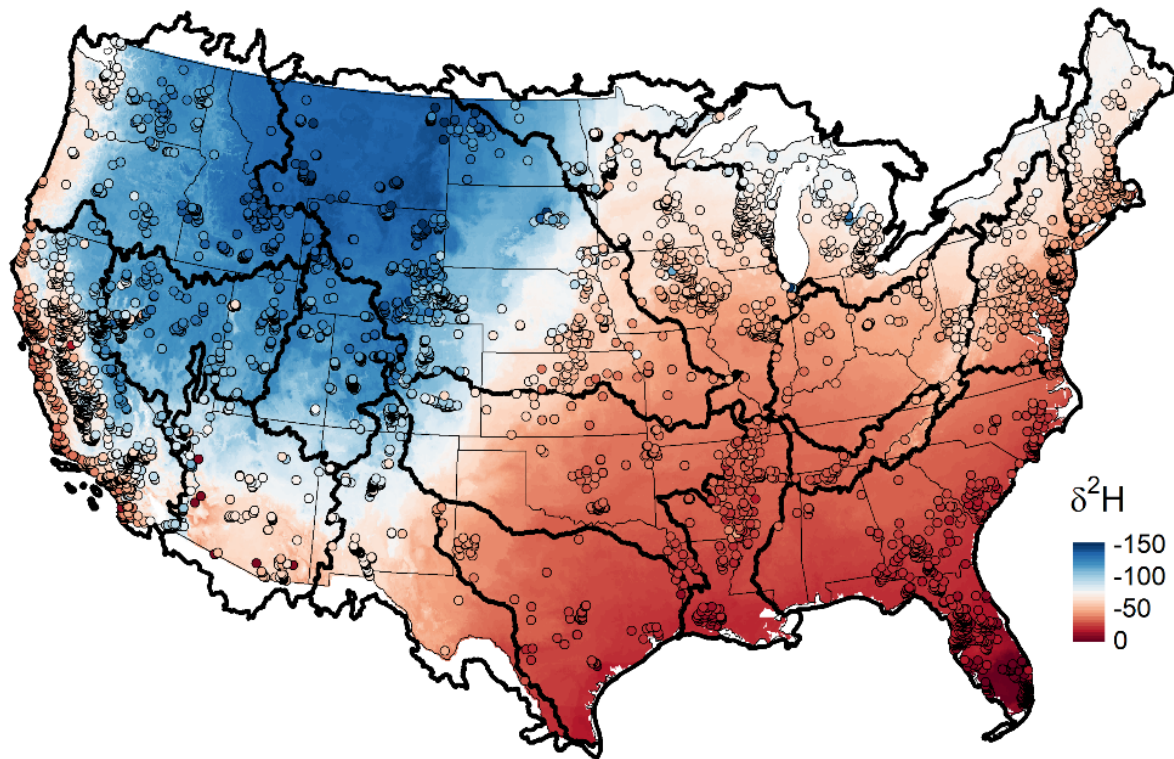


Figure 19. The interpolated surface generated for $\delta^2\text{H}$ in groundwater using the Random Forest model (Stahl et al., 2020). Observed values for isotopes are displayed as points. The important predictor variables in this model are annual weighted precipitation isotopes, elevation, annual precipitation amount, longitude, and latitude.

A steep gradient in isotope ratios is observed in California, with isotope values decreasing from -40‰ to -100‰ and 6‰ to -14‰, for $\delta^2\text{H}$ and $\delta^{18}\text{O}$, respectively, moving from the coast into the Sierra Nevada. In the eastern United States, the groundwater generally reflects isotopes of mean annual precipitation (Stahl et al., 2020).

3.4 DISCUSSION

We use the kriging approach on our groundwater data to apply a traditional method of predicting spatial values. While the kriging approach is widely used because of its simple application, this method has many limitations. The model is entirely dependent on the distance between two points, and does not take any other environmental parameters into account. The kriging approach is thus implicated in that it takes no additional information to predict any given point, providing a purely spatial correlation. Although this method provides a preliminary isoscape, we determine this method to be less defensible than the random forest model based on these limitations.

We favor the random forest model compared to the kriging approach. The random forest model is based on predictor variables which influence groundwater isotopes. We computed a measure of spatial correlation on our RF model residuals and found minimal spatial correlation (Moran's I for model residuals for $\delta^2\text{H}$ and $\delta^{18}\text{O}$ were $1.01 \cdot 10^{-2}$ and $2.69 \cdot 10^{-3}$, and p-values were $1.19 \cdot 10^{-12}$ and 0.027, respectively). Further, this model is advantageous as it ranks these variables in order of importance. Because of the significance of seasonal precipitation isotopes in the RF model, recharge seasonality can be interpreted as a dominant influence on groundwater isotopic values for $\delta^2\text{H}$ and $\delta^{18}\text{O}$. We observe a pattern which generally follows the precipitation isotope signals, as groundwater isotope values decrease moving from low-latitude and low-elevation regions to more continental, high-latitude, and mountainous areas. We compare our modeled groundwater $\delta^2\text{H}$ using the random forest model to annual amount weighted precipitation $\delta^2\text{H}$ values (Figure 20).

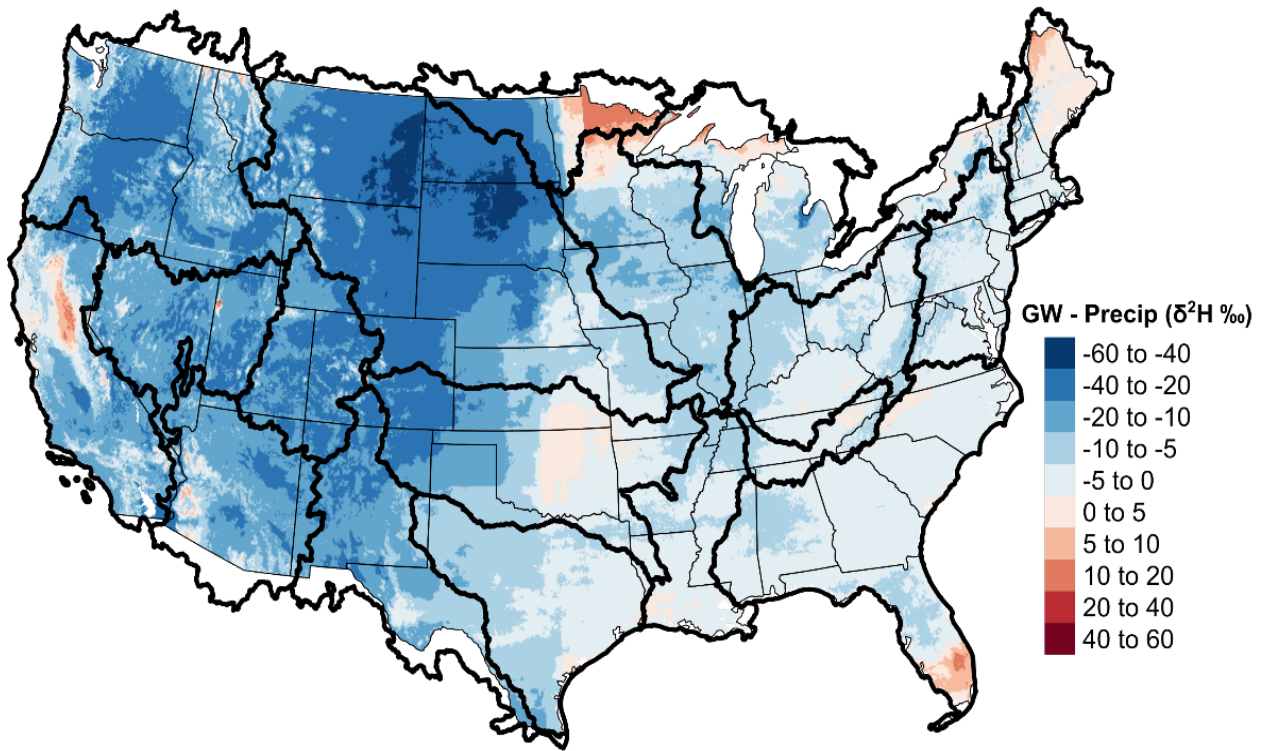


Figure 20. Difference between modeled groundwater and annual amount weighted precipitation for $\delta^2\text{H}$ (Stahl et al., 2020). HUC02 regions are outlined in black.

We observe similar (within 10‰) groundwater and mean annual precipitation isotopes for regions east and around the Mississippi River, suggesting groundwater could be a proxy for precipitation in this region. Groundwater is depleted relative to mean annual precipitation isotopes (less than -10‰) west of the Mississippi River through the mountainous regions in the west, perhaps due to larger seasonal differences in precipitation isotopes compared to the Eastern United States. Larger deviations indicate groundwater isotopes are not a viable proxy for precipitation isotopes in the Western United States.

3.5 CONCLUSIONS

We provide the first comprehensive groundwater isoscapes for the United States using two modeling approaches. The kriging method provides a traditional approach to predicting groundwater isotopes, as the interpolated surface is generated using the average isotopic composition of groundwater sites to extrapolate between spatial points. The random forest model provides a predictive model for groundwater isotopes by using environmental parameters to determine isotopic compositions. We observe similar trends for both of the isoscapes, including more negative values inland and more positive values along coastal regions. We favor the random forest model approach over the kriging method, as the RF model allows for predictions based on important environmental factors. In addition, this method is useful for quantifying the relationships between these variables to track the most important factors influencing stable isotopes of groundwater. The overall performance of the predictive model provides further confidence for use of this isoscape.

Groundwater isotopes provide insight into hydrological processes affecting groundwater systems and thus are important to understand for sustainably managing water resources. A continuous predictive surface for shallow groundwater isotopes can be used for a variety of hydrologic, ecologic, and forensic applications. We utilize our isoscape to observe spatial patterns in groundwater isotopes and compare the relationship of these values to precipitation isotopes, thus indicating areas for which groundwater isotopes may serve as a proxy of precipitation isotopes. Other applications for the groundwater isoscape in hydrology includes estimates of baseflow, as baseflow in rivers and streams is often fed by shallow groundwater systems; isotopes can be used to quantify baseflow inputs to streams once isotopic hydrograph separations are determined. Because biological features (including hair, feathers, leaf water, and

animal tissue) are influenced by groundwater isotopes, this isoscape could serve as an input for ecological models. Forensic applications include the identification of the sourcing of water, including tap or bottled water (Bowen et al., 2005; Jameel et al., 2016), and the sourcing of plant and animal tissues (West et al., 2010). Thus, in addition to providing estimates for groundwater isotopic measurements across the United States, we demonstrate the versatility and applicability of this isoscape across a variety of disciplines.

4 Surface Water and Groundwater Interaction Along the Mohawk River

4.1 BACKGROUND

A major focus of hydrologic and water resource research is the interaction between surface water and groundwater. Streamflow infiltration, where water is captured from streams or rivers and flows into an aquifer, is a function of water levels, hydraulic gradients of the subsurface, and streamflow rates. Pumping water from an aquifer reduces the water level in the aquifer and around the well-field, in a difference in the water level in the aquifer and surface water in the surrounding area. The head of water necessary to infiltrate the aquifer (and become extracted from the well-field) is represented by the difference between the river and aquifer levels. For wells adjacent to lakes or rivers, such as the Mohawk River, the water pumped from the aquifer can be infiltrated from the river. The transmissibility of the river and aquifer, as well as the hydraulic gradient between the adjacent well and river, determines the amount of water infiltrated (Winslow et al., 1965). While streamflow infiltration could be advantageous particularly in arid or semiarid environments where a continuous source of recharge may be lacking, there is a risk of contaminated river water being captured and transported into the well-field. The risk for contamination is related to how long it takes for water to move from the surface water body into the adjacent well-field (Winslow et al., 1965).

Schenectady County, included in the Capital District, is located in the Mohawk Valley in east-central New York (Simpson, 1952). The importance of groundwater in the area is demonstrated by the dependence of the majority of the county on the aquifer as the primary water supply. Extensive shallow sand and gravel deposits occupying buried Mohawk channels have provided millions of gallons of groundwater daily to Schenectady County since 1945 (Simpson, 1952; Waller and Finch, 1982). Increasing development in the area has provided the basis for the efficient utilization of groundwater resources.

The timescales of storage in catchments can be estimated using stable isotopes as tracers of seasonal cycles. The mean transit time describes the average time it takes for water to travel through a system and emerge. Kirchner (2016) applied sine-wave fitting to seasonal signals from precipitation and stream isotopes to determine the timing of precipitation travelling through the catchment system and emerging as streamflow. The fraction of young water describes the proportion of water that is sourced from that which has been recently recharged (DeWalle et al., 1997; Kirchner, 2016). This study applies these concepts—extending the application by moving from a source into the reservoir. Because contaminant behavior (retention and release) is dependent on catchment system timing, this application highlights the connection between the Mohawk River and the aquifer in the vicinity of the Schenectady well-field.

4.1.1 Geologic Setting

There are six primary geologic units identified in Schenectady County: bedrock, glacial till, outwash sand and gravel, glacially-deposited sand, silt and clay, and alluvial sand, respectively (Johnson, 2009). Underlying rocks in Schenectady County were deposited in early Paleozoic time and late in the Cenozoic. Paleozoic rocks, deposited in shallow Ordovician seas, consist of alternating beds of shale and sandstone. In the eastern part of the county, crustal deformation caused rocks to be folded and faulted (Simpson, 1952); limestone beds in the southwestern part of the county make up the Schenectady Formation, resulting in the simple structure of consolidated rocks (Winslow, 1962; Halberg et al., 1964). The overflow of the glacial Great Lakes discharging through the Mohawk and Hudson Valleys deposited outwash sand, gravel, and clay, which mantles the bedrock. Unconsolidated glacial drift, deposited during the Pleistocene, is the result of the advance and retreat of the continental ice sheet

(Simpson, 1952; Figure 21). The Mohawk River, which flows eastward from Schenectady, accounts for most of the drainage in Schenectady Country to the Hudson River (Halberg et al., 1964).

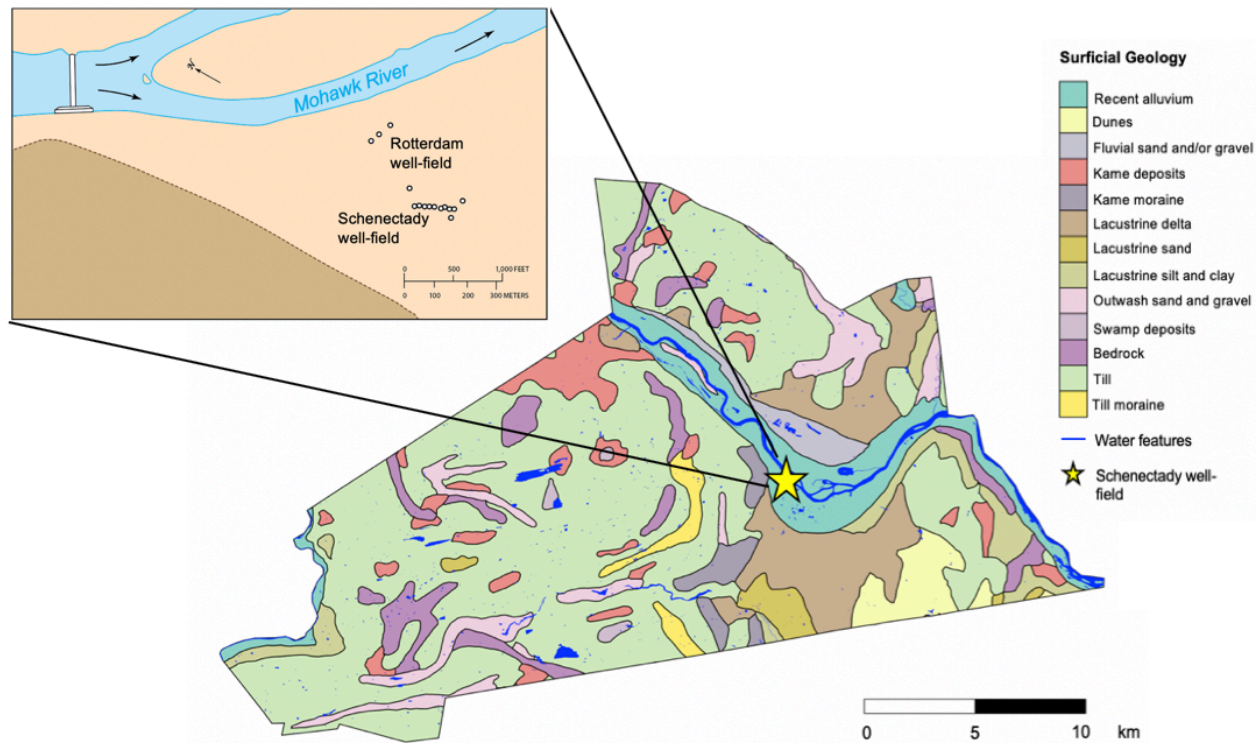


Figure 21. Map of surficial geology in Schenectady County, New York, highlighting the principal unconsolidated deposits (NYS Education Department). The location of the Schenectady well-field is depicted (star). The inset figure shows the position of the Schenectady well-field adjacent to the river at Lock 8 (*modified from Barlow and Leake, 2012*).

The Great Flats aquifer consists of highly permeable sand and gravel deposits overlain by silt deposits (Waller and Finch, 1982; Barlow and Leake, 2012). Recharge in the aquifer is controlled mainly by precipitation (directly on land) and seepage from streams. In addition, recharge from the Mohawk River is attributed to limiting the susceptibility of the Schenectady, Rotterdam, and Glenville well fields to potential drought conditions (Johnson, 2009). The aquifer principally discharges to the Mohawk River and wells in the adjacent well-field (Waller and Finch, 1982). The Schenectady well-fields are sited nearly one kilometer from the Mohawk

River, making the interaction between surface water and groundwater highly complex and seasonally dependent. Aquifer pumping induces fluctuations of surface water and groundwater temperatures in this system due to infiltration from the river (Barlow and Leake, 2012). Where flow is induced from the river into the aquifer from pumping (in the adjacent Schenectady, Glenville, and Rotterdam well fields), the aquifer is recharged—classified as a reversal of the typical relationship between the river and the aquifer systems (Johnson, 2009).

4.1.2 Water Supply

Approximately 4,000 feet from lock 8, a dam and navigation lock along the canal, the Schenectady and Rotterdam well fields are sited along the flood plain of the Mohawk River. At lock 8, the most productive water-bearing area along the Mohawk River flood plain, gravel beds are nearly 100 feet thick (Winslow, 1962). At the Schenectady well-field, the thickness of the sand and gravel aquifer is about 30 feet. Sand and gravel transition to fine-grained sand beyond the well-fields (Winslow, 1962; Halberg et al., 1964).

Utilization of the Great Flats Aquifer began in 1897 in the city of Schenectady, with three wells at approximately 50-foot depths. The Great Flats aquifer is the primary source of water for Schenectady County, pumping water through a system of approximately 12 wells. The public water supply in Schenectady currently serves approximately 62,000 people in the county and a small portion of the neighboring towns of Niskayuna and Rotterdam. In 2018, the aquifer produced 4,490,070,480 gallons of water, with a daily average of 12,298,330 gallons (Department of Water, 2018).

Artesian conditions exist locally in Schenectady County in the gravel deposits along the Mohawk River flood plain; downstream of Schenectady, widespread confining beds exist as a

result of irregularly spaced layers of silt and clay. The water table, or the upper surface in the zone of saturation, in Schenectady generally conforms to the land surface (Simpson, 1952).

Responses of the water level in the aquifer to changes in the stage of the Mohawk River—instead of seasonal fluctuations—has been demonstrated since 1946 (Simpson, 1952; Barlow and Leake, 2012). Because of the control of canal locks on the water level in the Mohawk River, the water level in the aquifer fluctuates between navigational and non-navigational seasons (Johnson, 2009). Thus, well fields proximal to the Mohawk River are not as susceptible to drought conditions in the summer.

Clear, clean water is produced by the Great Flats Aquifer; besides the relative hardness of the water (which has decreased since wells have first been tapped), there are no contaminants reported (Allen and Waller, 1981). The pH of water from sand and gravel localities ranges from 6.6 to 8.3. Temperatures of the water from the Schenectady supply wells range from 40°F to 65°F (Simpson, 1952). Well water is disinfected with a chlorine residual (0.2 mg/L) prior to distribution, following standard procedures. There are no current restrictions on this water source (Department of Water, 2018). Streams draining into the Mohawk River have been established as potential sources of contamination to the aquifer (Allen and Waller, 1981).

Given the importance of the Great Flats Aquifer to the Capital region, groundwater availability and quality are monitored (Simpson, 1952; Allen and Waller, 1981). In a broad sense, river monitoring systems along the Mohawk River are useful indicators for aquifer protection (Allen and Waller, 1981). The potential effects of increased groundwater withdrawal have been proposed for this well field, as increasing population and development has highlighted the dependence of the County for clean, readily available water (Johnson, 2009). The lack of a complete analysis on groundwater and surface water conditions in the vicinity of Schenectady

necessitates a greater understanding of the hydraulic connection between the Mohawk River and the well field.

4.2 METHODOLOGY

4.2.1 *Field Methodology*

Schenectady tap water, supplied by the Schenectady well-field, and Mohawk River water were collected at regular intervals to understand seasonality and municipal water sourcing. Tap water samples, which reflect regional groundwater, are collected in duplicate in 15 mL Falcon tubes at Union College (Olin 015). Mohawk River water samples are collected using an extender pole and tubing at Freeman's Bridge in Schenectady, New York. Tubing is flushed with river water prior to sample collection; samples are taken 6 feet from the dock at a depth of approximately 2 feet below the surface. All tap water and river water samples are parafilmmed and refrigerated immediately after sampling.

4.2.2 *Laboratory Methodology*

The tap water samples were analyzed for $\delta^{18}\text{O}$ values using a Thermo Gas Bench II connected to a Thermo Delta Advantage mass spectrometer in continuous flow mode, and $\delta^2\text{H}$ values using a Thermo TC/EA at 1425°C connected via a ConFlo IV to a Thermo Delta Advantage mass spectrometer in continuous flow mode. Both analyses were conducted at Union College in the Stable Isotope Lab. Three inhouse laboratory standards were used for isotopic corrections for measurements of $\delta^{18}\text{O}$, and to assign the data to the appropriate isotopic scale using linear regression. These standards were calibrated directly to VSMOW (0.0‰) and SLAP (-55.50‰). The inhouse standards have $\delta^{18}\text{O}$ values that range from -0.6‰ to -16.52‰. The combined uncertainty (analytical uncertainty) for $\delta^{18}\text{O}$ is $\pm 0.01\text{‰}$ (SMOW), based on 3 internal

tap water standards over one analytical session. For $\delta^2\text{H}$ measurements, each sample was analyzed six times by injecting 100 nL into the TC/EA using a CombiPAL autosampler. To remove the memory effect, only the last four analyses of each sample were averaged. Three in-house standards were used for isotopic corrections, and to assign the data to the appropriate isotopic scale using linear regression. These standards were calibrated directly to VSMOW (0.0‰) and SLAP (-427.5‰). The inhouse standards have $\delta^2\text{H}$ values that range from -4.5‰ to -121.4‰. The combined uncertainty (analytical uncertainty) for $\delta^2\text{H}$ is $\pm 0.67\text{‰}$ (VSMOW), based on 7 tap water standards over 2 analytical sessions.

4.2.3 *Hydrologic Analysis*

The majority of relationships derived from isotopic studies originate from stream, river, and precipitation samples, as surface waters provide relatively sensitive information for movement on short-time scales (Dutton et al., 2005). Locally, the Schenectady well-field induces recharge from the river to the aquifer; to characterize the surface water and groundwater interaction within the vicinity of the Schenectady well-field, we compare time-series data of tap water isotopes to that of the Mohawk River. The Mohawk River exhibits strong seasonal patterns in $\delta^2\text{H}$ and $\delta^{18}\text{O}$ and this isotopic signal can be compared against the signal of the Schenectady tap water (groundwater).

As water is transmitted through catchments, the seasonal cycles in precipitation are damped and phase-shifted (Figure 22).

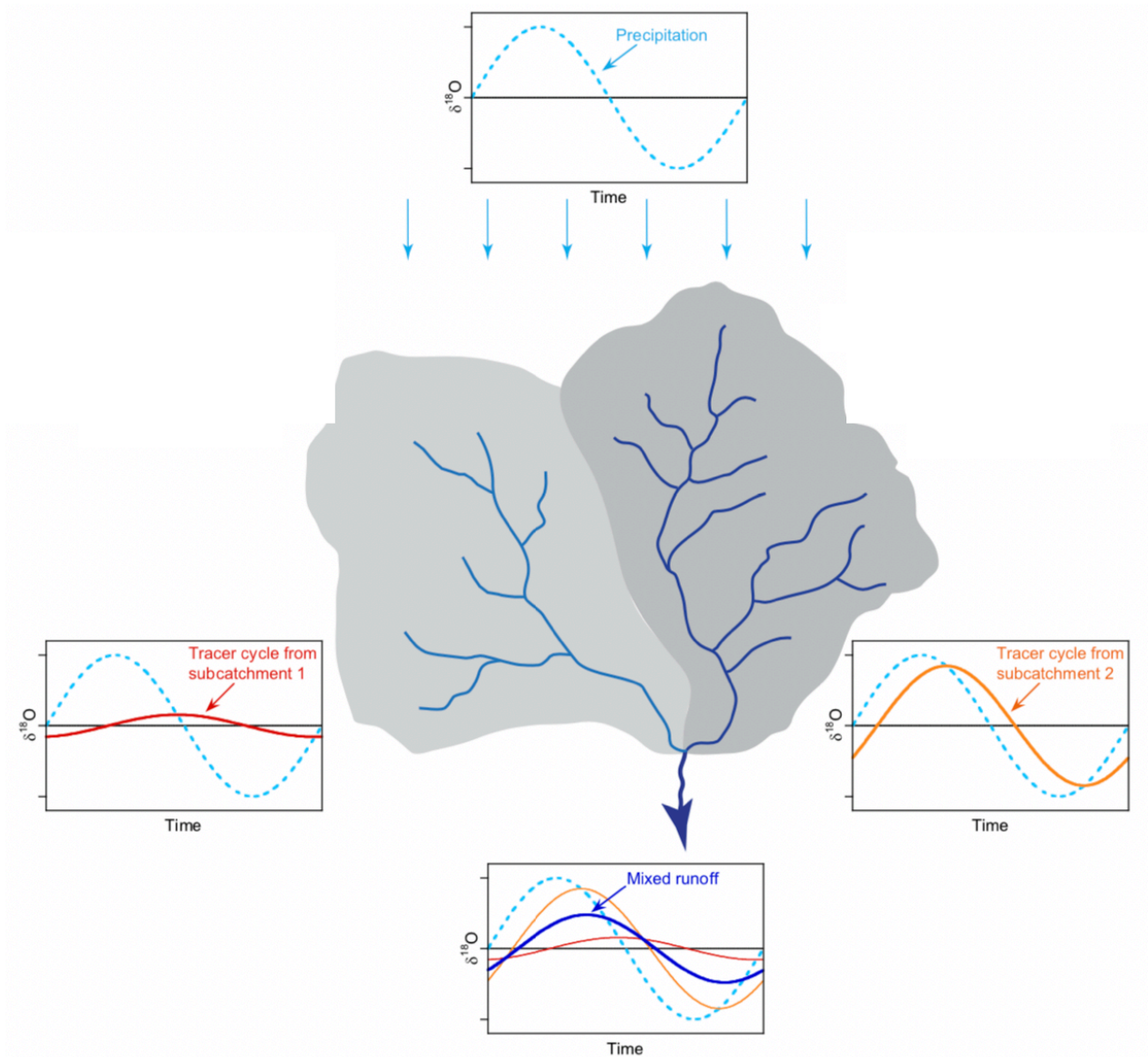


Figure 22. Model of the input and output signals from isotopes, modified as water traverses through the catchment system (modified from Kirchner, 2016). Here, the input signal is precipitation and the output signal is surface waters.

Kirchner (2016) demonstrates the use and limitations of environmental tracers to understand how watersheds modify the input signal of precipitation and generate the output signal in streamflow. The basis of sine-wave fitting is validated by the amplitude (A) of groundwater being damped and phase-shifted (ϕ) relative to river water. The transit timing of water and the proportion of

young water are based on such differences between the input and output signals. Dampening explains the proportion of mixing, or the fraction of water less than 2.7 months old. The fraction of young water is determined by the ratio of amplitudes:

$$FY = \frac{A_{\text{tap}}}{A_{\text{river}}}$$

where FY is the fraction young water and A is the amplitude of the tap water and river water peaks. The phase shift calculates how long on average it takes for the seasonal signal in the river to make its way to the groundwater. The mean transit time is calculated by the differences in the phase:

$$MTT = \varphi_{\text{tap}} - \varphi_{\text{river}}$$

where MTT is the mean transit time and φ is the phase of the tap water and river water. For heterogenous catchments, calculating the dampening of the amplitude and the phase lag on the input signal can lead to over-estimates for mean residence times (Farlin and Małoszewski, 2016; Kirchner, 2016). Because subsurface systems react slowly to precipitation events, the seasonal cycle of isotopes can be used for dating purposes without such implications (Farlin and Małoszewski, 2016).

We use a similar approach to Kirchner (2016), utilizing the seasonal signals of tap water (groundwater) and river water to track water through the reservoirs—as opposed to the source (precipitation). We assume water in the system is less than 1 year, based on the idea that the sine-wave signal is a convolution of many signals. Because the super position of the signals generates the output, amplitude dampening sets the age thresholds (Kirchner, 2016). By comparing the amplitudes of the isotopes signals in the river and tap water, we determine the proportion of tap water sourced from recently (< 2.7 months) recharged river water (Maloszewski et al., 1984; DeWalle et al., 1997; Kirchner, 2016). We also examined the shift in

phase of the isotopic signal in the tap water to that of the river water to determine the average linear velocity of the groundwater on its path from the river bank to the municipal wells. These calculations provide the basis for understanding the timing and the relative age of the flow of water from the river to the aquifer (Figure 23).

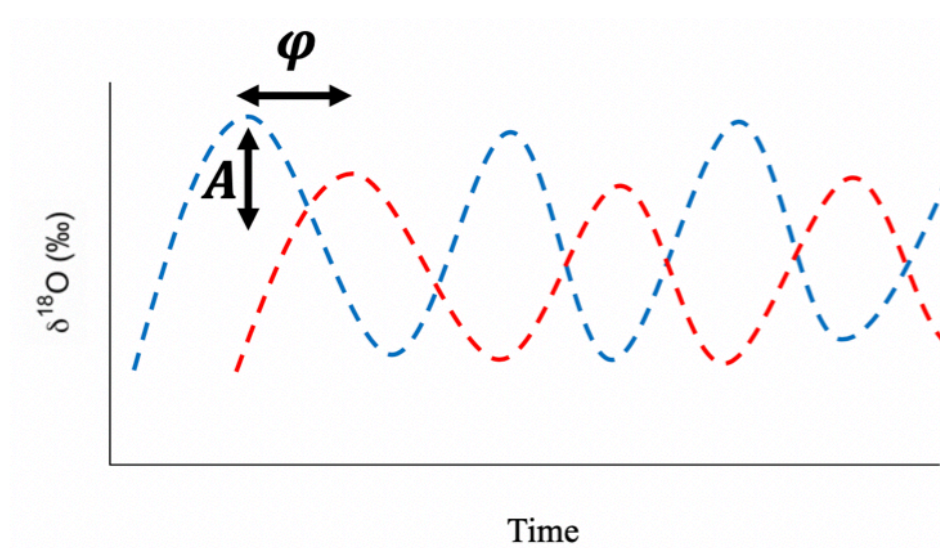


Figure 24. Demonstrates the use of time-series data for insight into hydrologic processes; amplitude (A) and phi (phase shift) values are shown. The blue line represents the hypothetical “input” signal (river water) and the red line indicates the hypothetical “output” signal (groundwater).

4.3 RESULTS

The $\delta^2\text{H}$ and $\delta^{18}\text{O}$ of local river and groundwater generally fall along the LMWL, and above the GMWL (Figure 24).

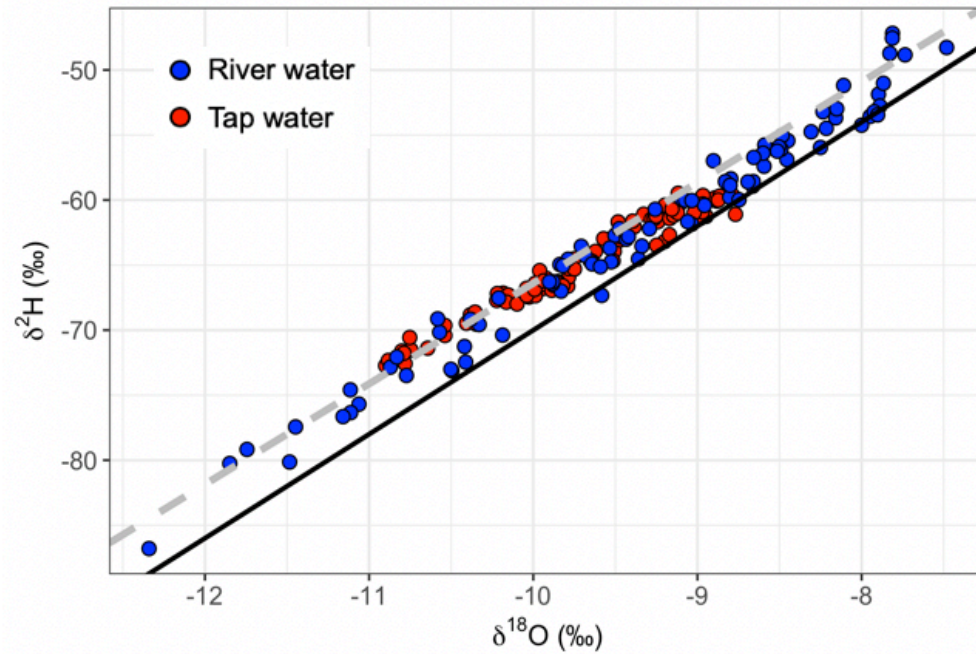


Figure 24. Results of isotopic analyses show that $\delta^2\text{H}$ and $\delta^{18}\text{O}$ values of local river and groundwater generally fall along the LMWL (grey line; the black line represents the GMWL).

Fitting a sine wave through time series data of $\delta^{18}\text{O}$ values (Figure 25) yields amplitudes of 0.732‰ and 1.274‰, for tap water and river water, respectively.

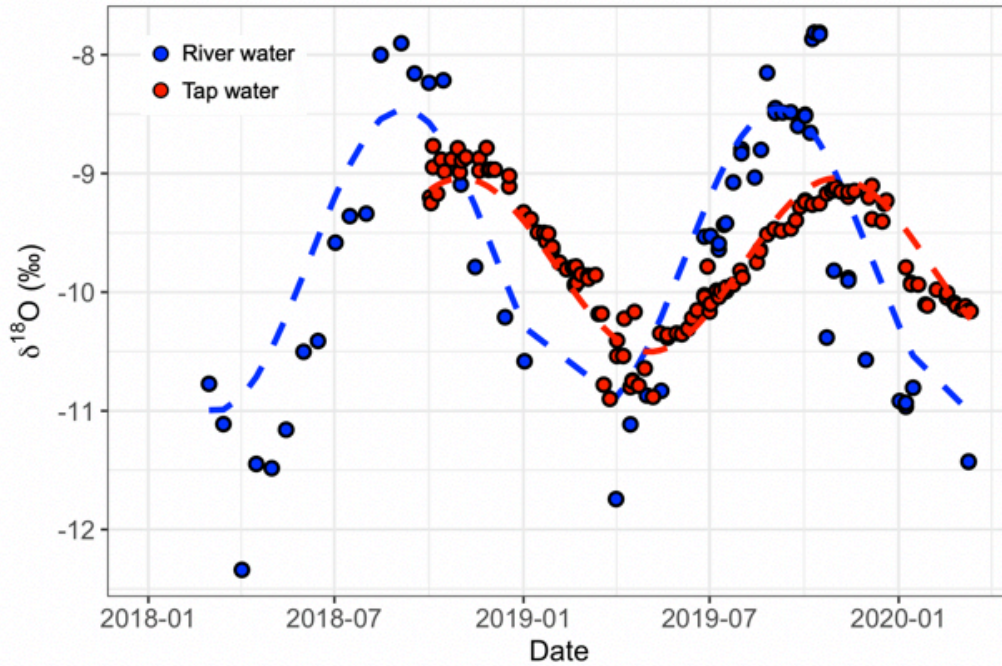


Figure 25. Time-series data for isotopic compositions of river (blue) and tap (red) water. Fitting a sine wave yields amplitude and phase values for river and tap water.

The ratio of the amplitudes is 0.574. The sine wave yields phase (ϕ) values of -30.375 and -28.671 for tap water and river water, respectively (Table 4). The difference in phase between river water and tap water is approximately 3.2 months (99 days).

Table 4. Values for amplitudes and phase given by the fitted sine wave for measurements of $\delta^{18}\text{O}$ in the Mohawk River water and Schenectady tap water.

Water Source	A (‰)	ϕ (‰)
Tap	0.732	-30.375
River	1.274	-28.671

We evaluate the sine-wave fit for tap water and river water by comparing the values of measured $\delta^{18}\text{O}$ to those of the modeled $\delta^{18}\text{O}$ (Figures 26 and 27).

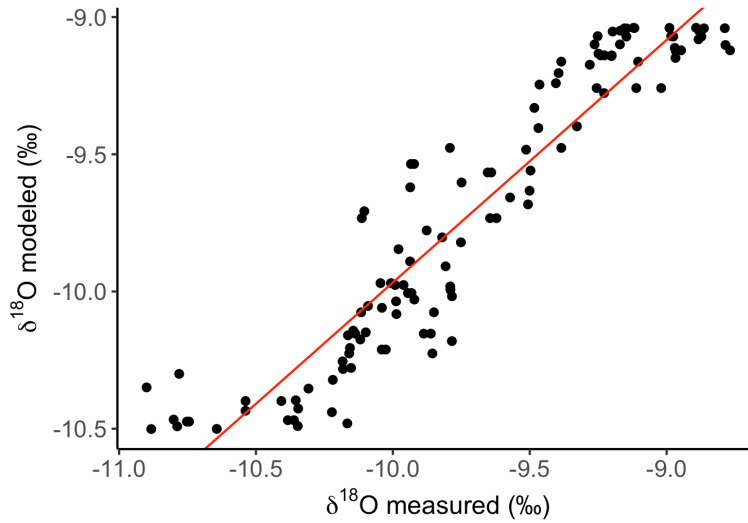


Figure 26. Displays how well the sine-wave fit describes the observed measures for tap water ($r^2 = 0.88$).

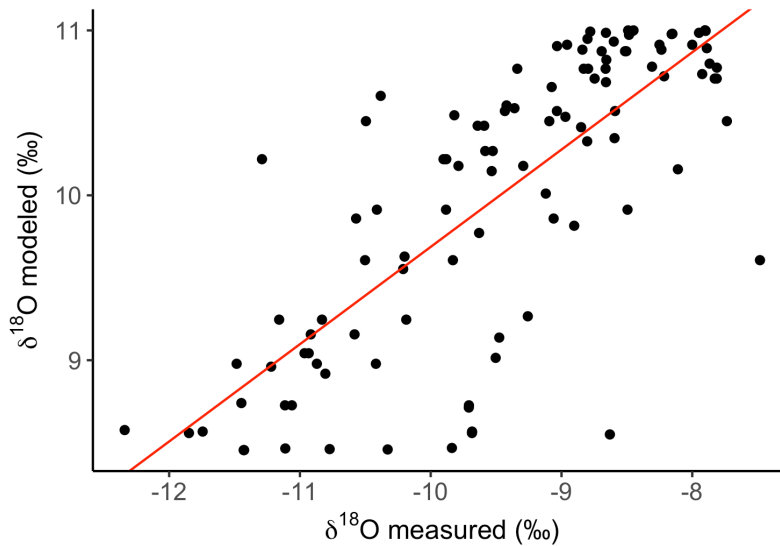


Figure 27. Displays how well the sine-wave fit describes the observed measures for river water ($r^2 = 0.59$).

The r^2 values for the uncertainty estimates for tap water and river water are 0.88 and 0.59, respectively. We attribute the greater uncertainty in the river water to the relative scarcity of samples compared to tap water. We are confident the error associated with values for amplitude

demonstrate less uncertainty than those associated with phase. These ratios represent the fraction of young water in the system and the average time it takes for water to traverse from the Mohawk River into the aquifer, allowing for the interpretation of isotopic tracer signals (DeWalle et al., 1997; McGuire and McDonnell, 2006). A range of values was calculated for the fraction of young water and the mean transit times using standard deviations and upper and lower bounds for the hydraulic conductivity of the aquifer and distances from the river to the well-field (Figures 28 and 29).

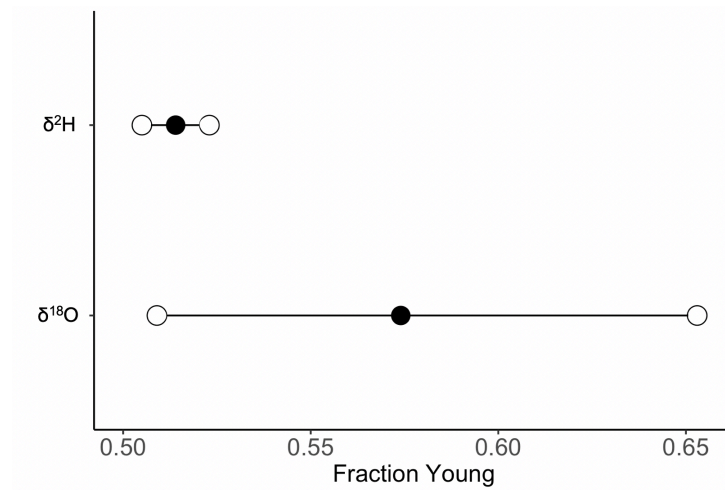


Figure 28. Range of fraction young calculations for the amplitudes of river and tap water for $\delta^2\text{H}$ and $\delta^{18}\text{O}$. The range is calculated by using the upper and lower bounds for standard deviations.

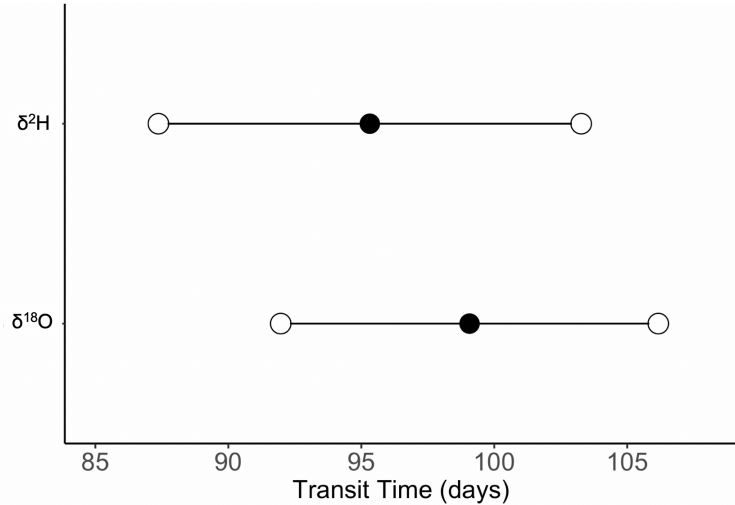


Figure 29. Range of mean transit times calculated for the phase of river and tap water for $\delta^{2}\text{H}$ and $\delta^{18}\text{O}$. The range is calculated using the upper and lower bounds for standard deviations.

4.4 DISCUSSION

4.4.1 *Fraction Young and Mean Transit Timing*

Time-series data for the isotopic compositions of river and tap water reveal a phase lag and dampening effects, as the values for tap water are shifted from river water values and the peaks are dampened (Kirchner, 2016). The fraction of young water, determined by the ratio of the amplitude of tap water to the amplitude of the river water signal, is 0.57—indicating 57% of the water transported from the river to the aquifer is young water, or water that is less than 2.7 months old. Thus, nearly 60% of the water supply for Schenectady is recently (less than 2.7 months prior) supplied by the Mohawk River. We calculate the average time it takes for water from the river to reach the aquifer to be 3.2 months, giving an average linear velocity of approximately 3.53 m/day. Understanding water transport and flow conditions provides insight into the vulnerability of water sources and water quality, as the rate of transport may be used to

predict the movement of contaminants introduced to the Mohawk River—and thus traversing into the aquifer (or vice versa).

The movement of contaminants near the aquifer is greatly influenced by the extent and distribution of groundwater pumping. The Mohawk River has the highest potential for introducing contamination into the well-field. Potential areas which could induce contamination into the river in Schenectady County include chloride leachate from road salts and polluted runoff from industrial complexes along the adjacent highway (Allen and Waller, 1981). Because water flowing down the Mohawk River has the potential to leave and re-enter the aquifer, the complexity of contaminant transport is perhaps oversimplified (Allen and Waller, 1981). Regardless, isotopic measurements suggest a contaminant transported by water from the river would take 3.2 months on average to reach the well-field—not considering the amount, type, or solubility of the theoretical contaminant.

Winslow et al. (1965) calculated the travel times from the Mohawk River into the Schenectady well-field based on temperature gradients of approximately 41 to 43 days—a difference from our calculations by at least a factor of 2. We attribute this more rapid travel time to higher pumping rates and a higher water demand in Schenectady during the 1960s. From 1960 to 1961, Winslow et al. (1965) reported pumping rates between 16 and 25 million gallons of water per day, indicating an approximate 25-52% decrease in pumping rates from the 1960s to today. Higher pumping rates would have induced a greater change in the water levels of the aquifer, increasing the rate of infiltration from the river to the adjacent well-field and thus result in a more rapid travel time than calculated today. Despite the variation in travel times reported here and in 1965, the resulting travel times still indicate the flow path from the river into the aquifer could permit polluted water to enter the well-field.

4.4.2 Physical Hydrology

We evaluate the calculated values for average linear velocity using Darcy's Law to determine if such values given by the isotopic measurements imply reasonable physical hydrology. Darcy's Law is given by the following equation:

$$Q = KA \frac{dh}{dl},$$

where Q is the volumetric flow rate [L³/T], K is the hydraulic conductivity, A is the cross-sectional area [L²], and dh/dl is the hydraulic gradient [L/L] (Freeze and Cherry, 1979). Simpson (1952) reports the hydraulic conductivity of the Schenectady aquifer to be "tens of thousands of gallons per day per square foot of aquifer at unit hydraulic gradient." Thus, we constrain the hydraulic conductivity in the Schenectady aquifer to be between 400 m/day (lower limit) and 4,000 m/day (upper limit). The hydraulic gradient that would result using our estimation of the average velocity of water flowing from the river to the well-field is calculated as follows:

$$\frac{dh}{dl} = \frac{q}{k},$$

where dh/dl is the hydraulic gradient, q is the average linear velocity, and k is the hydraulic conductivity. The results of this calculation, using lower and upper bounds for hydraulic conductivity and linear velocity (determined by minimum and maximum distances from the well-field to the river), are displayed in Table 5.

Table 5. Calculated head gradients using upper and lower bounds for average linear velocities and hydraulic conductivity.

	K _L (400 m/day)	K _U (4,000 m/day)
q _L (3.53 m/day)	8.83 × 10 ⁻³	8.83 × 10 ⁻⁴
q _U (10.09 m/day)	2.52 × 10 ⁻²	2.52 × 10 ⁻³

The resulting head gradients varied from $\frac{8}{1000}$ to $\frac{2}{100}$; that is, for the lower bound estimations, there is 8 meters of vertical displacement for every 100 meters of length. Upper bound estimations result in 2 meters of vertical displacement for every 100 meters of distance (Table 5). Although lower constraints result in steep head gradients, all of the estimated values are physically feasible for rivers adjacent to pumping wells (Freeze and Cherry, 1979). Simpson (1952) demonstrates the relation between water levels in the Mohawk River and the groundwater. During the non-navigational season (April to Mid-December), the average river level is 214 feet, while the average groundwater level at a Schenectady supply well is 208 feet. The average difference between the two levels is approximately 6 feet. Given the hydraulic gradient represents the change in the head gradient over length, the hydraulic gradient for the river stage and groundwater stage is $\frac{6}{1000}$, and becomes shallower moving further down the river (Simpson, 1952). In comparison, our calculations for the hydraulic gradient agree with Simpson's (1952) findings.

The validation of transit timing estimations further proves the significance of such a method. In other hydrologic studies, calculating groundwater velocities requires many measurements—several of which are difficult to acquire over time. Measurements for hydraulic conductivity in a given aquifer require pumping tests for water systems, and accurate water level data requires years of acquired field measurements (Simpson, 1952; Allen and Waller, 1981). Estimating how long on average it takes water to move from one reservoir to another using isotopic values provides less opportunity for error than other methods, as the only error associated is analytical. This method provides the means for understanding where water

originates, the risk of groundwater contamination from induced recharge from surface water sources, and the potential for groundwater pumping to impact adjacent surface water bodies.

4.5 CONCLUSIONS

Groundwater and surface water are a conjunctive resource. We have demonstrated the use of stable isotopes to characterize the mean transit time and fraction young water by fitting sine-waves to the seasonal isotopic signal (Kirchner, 2016). Our results highlight the connection between the Mohawk River and the aquifer near the Schenectady well-field. Pumping from the Schenectady well-field induces recharge from the Mohawk River; this water ultimately reaches the well-field, where it is extracted for municipal water use. Given river water “has easy access to the aquifer through the river bed near lock 8,” there are implications for water quality should a contaminant be introduced and traverse into the aquifer (Simpson, 1952). Groundwater pulled into the well-field from the river can be used to determine how fast water is moving in the system, and can thus indicate how long it would take for a contaminant to break down before it gets to the well-field. We calculate an average linear velocity of 3.53 m/day, which describes how long on average it takes for water to traverse through the system. Additionally, we constrain the fraction of young water, and find that nearly 60% of the municipal water supplied by Schenectady is from river water that entered the aquifer less than 2.7 months earlier. This method is further validated by estimating plausible hydraulic gradients using our values for the average linear velocity, proving this technique can be used to understand water supply vulnerabilities and the complex interaction between groundwater and surface water in this region.

Regionally a significant proportion of municipal well-fields are sited less than a kilometer from rivers (Hettiarachchi et al., 2016). We demonstrate the opportunity for this method to be applied to similar systems to understand how long it takes water to get into the aquifer, and thus deduce infiltration rates in these areas (Hettiarachchi et al., 2016; Kirchner, 2016). Should seasonal changes result in changes in viscosity, it is possible lag timing could change depending on seasonality; thus, more subtle variations in stable isotopes should be considered throughout water systems (McGuire and McDonnell, 2006). Future research on the interactions between groundwater and surface water will be particularly significant, as future challenges in water resources (e.g. climate, extreme weather, and energy for food and industry) intensify pressure on freshwater availability and quality.

5 Conclusions

5.1 SUMMARY

Characterizing hydrological processes and establishing connections between water distribution systems and their respective environmental sources is possible through the use of stable water isotopes ($\delta^2\text{H}$ and $\delta^{18}\text{O}$). Characterizing recharge processes across the United States provides insight into the seasonal timing of recharge and the environmental or climatic factors which influence these processes, and what this implies for the sustainability of groundwater resources. For most sites across the U.S., we observe winter recharge (October-March) is more efficient than summer recharge (April-September). Along the coast of California, our results suggest fog drip contributes to groundwater recharge, necessitating further research in areas where fog may be an importance source of recharge to aquifers.

In addition, we develop groundwater isoscapes for the contiguous U.S. using two different approaches: kriging and random forest modeling. The random forest model is more robust than the kriging approach based on its prediction for groundwater isotope values using environmental parameters which influence isotopic values. The development of this isoscape can be used to combat the pre-existing limitations where there is no such groundwater data, and will have applications across environmental sciences and disciplines.

To further demonstrate the versatility of groundwater isotopes, we collected river water and tap water in Schenectady, New York, to disentangle the interaction between surface water and groundwater. We approximate the seasonal signal of isotopes using sine-waves, and calculate the mean transit time (3.2 months) for water traveling from the river into the aquifer and fraction of young water (57% < 2.7 months). Our results highlight the possibility for streamflow infiltration to permit polluted water to enter the well-field through the aquifer

adjacent to the Mohawk River. Together, these projects highlight the use of stable water isotopes across continent-wide and local scales.

5.2 FUTURE RESEARCH

Groundwater is an essential resource for both drinking water and the industrial food supply and serves a critical ecological and hydrological role in the environment. Here, we have demonstrated the applicability of stable water isotopes to understand the seasonal timing of groundwater recharge, the spatial distribution of isotopes and influential environmental factors on such isotopic compositions, and the complex interactions and vulnerabilities that exist between groundwater and surface water. These projects have been motivated by threats to groundwater resources, as future challenges in groundwater quality and management, including climate change, more frequent and intense weather events, and groundwater depletion, require a deeper understanding of water systems. Future research to constrain the potential effects of climate and increased water use on groundwater is necessitated, as these effects will induce changes to groundwater availability and quality. We have demonstrated the potential for similar studies to implement isotopic research for the characterization of vulnerabilities in water supply systems where pumping has induced river flow into aquifers. This thesis provides insight into the use of chemical information as a low-cost and effective approach to characterize vulnerabilities and to improve our understanding of physical hydrologic processes that are impossible to characterize at broader scales from physical measurements alone.

6 References

- Allen, R.V., and Waller, R.M., 1981. Considerations for monitoring water quality of the Schenectady aquifer, Schenectady County, New York: Geological Survey Water Resources Investigations 80-103, 28 p. DHQ.
- Al-Mashagbah, A., Al-Adamat, R. and Salameh, E., 2012. The use of kriging techniques with in GIS environment to investigate groundwater quality in the Amman-Zarqa Basin/Jordan. *Research Journal of Environmental and Earth Sciences*, 4(2), pp.177-185.
- Balling Jr, R.C., 1985. Warm season nocturnal precipitation in the Great Plains of the United States. *Journal of climate and applied meteorology*, 24(12), pp.1383-1387.
- Barlow, P.M. and Leake, S.A., 2012. Streamflow depletion by wells: understanding and managing the effects of groundwater pumping on streamflow (p. 44). Reston, VA: US Geological Survey.
- Beisner, K.R., Anning, D.W., Paul, A.P., McKinney, T.S., Huntington, J.M., Bexfield, L.M. and Thiros, S.A., 2012. Maps of Estimated Nitrate and Arsenic Concentrations for Basin-Fill Aquifers of the Southwestern United States. US Geological Survey.
- Bowen, G.J., Cai, Z., Fiorella, R.P. and Putman, A.L., 2019. Isotopes in the water cycle: regional-to global-scale patterns and applications. *Annual Review of Earth and Planetary Sciences*, 47, pp.453-479.
- Bowen, G.J. and Good, S.P., 2015. Incorporating water isoscapes in hydrological and water resource investigations. *Wiley Interdisciplinary Reviews: Water*, 2(2), pp.107-119.
- Bowen GJ, Wassenaar LI, Hobson KA. 2005a. Global application of stable hydrogen and oxygen isotopes to wildlife forensics. *Oecologia* 143 (3): 337–348.
- Bowen GJ. 2019. Gridded maps of the isotopic composition of meteoric waters.

- Chambers DB, Kozar MD, Messinger T, Mulder ML, Pelak AJ, White JS. 2015. Water quality of groundwater and stream base flow in the Marcellus Shale Gas Field of the Monongahela River Basin, West Virginia, 2011–12.
- Clark, I. and Fritz, P., 1997. The environmental isotopes. *Environmental isotopes in hydrogeology*, pp.2-34.
- Clark, I.D. and Fritz, P., 2013. *Environmental isotopes in hydrogeology*. CRC press.
- Clark, I.D., Fritz, P., Quinn, O.P., Rippon, P.W., Nash, H., Al Said, S.B.B.G., 1987. Modern and fossil groundwater in an arid environment: a look at the hydrogeology of Southern Oman. In: *Symposium on Isotope Techniques in Water Resources Development, IAEA-SM 299/15*. International Atomic Energy Agency: Vienna. pp. 167–187.
- Clark, I., 2015. *Groundwater geochemistry and isotopes*. CRC press.
- Cicco BLA De, Hirsch RM. 2014. The dataRetrieval R package: 1–26.
- Corbin JD, Thomsen MA, Dawson TE, D'Antonio CM. 2005. Summer water use by California coastal prairie grasses: Fog, drought, and community composition. *Oecologia* 145 (4): 511–521.
- Dansgaard, W., 1964. Stable isotopes in precipitation. *Tellus*, v16.
- Dawson TE. 1998. Fog in the California redwood forest: Ecosystem inputs and use by plants. *Oecologia* 117 (4): 476–485.
- DeWalle, D.R., Edwards, P.J., Swistock, B.R., Aravena, R. and Drimmie, R.J., 1997. Seasonal isotope hydrology of three Appalachian forest catchments. *Hydrological Processes*, 11(15), pp.1895-1906.

- Doveri, M., Menichini, M. and Scozzari, A., 2015. Protection of groundwater resources: worldwide regulations and scientific approaches. In *Threats to the Quality of Groundwater Resources* (pp. 13-30). Springer, Berlin, Heidelberg.
- Dutton, A., Wilkinson, B.H., Welker, J.M., Bowen, G.J. and Lohmann, K.C., 2005. Spatial distribution and seasonal variation in $^{18}\text{O}/^{16}\text{O}$ of modern precipitation and river water across the conterminous USA. *Hydrological Processes: An International Journal*, 19(20), pp.4121-4146.
- Fan Y, Li H, Miguez-Macho G. 2013. Global Patterns of Groundwater Table Depth. *Science* 339 (6122): 940–943.
- Farlin, J. and Małoszewski, P., 2016. The potential uses of tracer cycles for groundwater dating in heterogeneous aquifers 2. *Hydrology and Earth System Sciences Discussions*, pp.1-9.
- Fox, E.W., Ver Hoef, J.M. and Olsen, A.R., 2020. Comparing spatial regression to random forests for large environmental data sets. *PloS one*, 15(3).
- Freeze R.A. and Cherry, J., 1979. *Groundwater*. Prentice-Hall, Hoboken, NJ.
- Galewsky, J., Steen-Larsen, H.C., Field, R.D., Worden, J., Risi, C. and Schneider, M., 2016. Stable isotopes in atmospheric water vapor and applications to the hydrologic cycle. *Reviews of Geophysics*, 54(4), pp.809-865.
- Gimond, M., 2017. *Intro to GIS and Spatial Analysis*.
- Halberg, H.N., Hunt, O.P. and Pauszek, F.H., 1964. *Water Resources of the Albany-Schenectady Troy Area New York*. US Government Printing Office.
- Heath, R.C., 1984. *Ground-water regions of the United States (Vol. 2242)*. US Department of the Interior, Geological Survey.

- Hettiarachchi, H. and Ardakanian, R. eds., 2016. Safe use of wastewater in agriculture: Good practice examples. United Nations University, Institute for Integrated Management of Material Fluxes and of Resources (UNU-FLORES).
- Hijmans, R. 2019. raster: Geographic Data Analysis and Modeling. R package version 2.8-19.
- Iles DL, Rich T. 2017. Examination of Isotopes in Selected Waters in Eastern South Dakota. Vermillion.
- Ingraham NL, Matthews RA. 1990. A stable isotopic study of fog: the Point Reyes Peninsula, California, U.S.A. *Chemical Geology: Isotope Geoscience Section* 80 (4): 281–290.
- Ingraham NL, Matthews RA. 1995. The importance of fog-drip water to vegetation: Point Reyes Peninsula, California. *Journal of Hydrology* 164 (1–4): 269–285.
- Jasechko, S., Birks, S.J., Gleeson, T., Wada, Y., Fawcett, P.J., Sharp, Z.D., McDonnell, J.J. and Welker, J.M., 2014. The pronounced seasonality of global groundwater recharge. *Water Resources Research*, 50(11), pp.8845-8867.
- Jasechko, S., Kirchner, J.W., Welker, J.M. and McDonnell, J.J., 2016. Substantial proportion of global streamflow less than three months old. *Nature Geoscience*, 9(2), pp.126-129.
- Johnson, T.M., 2009. Responsible planning for future ground water use from the Great Flats Aquifer: Two Case Studies: The GEP Energy Project and the SI Green Fuels Boiler Project. Proceedings from the 2009 Mohawk Watershed Symposium, Union College, Schenectady NY.
- Kendall, C. and Coplen, T.B., 2001. Distribution of oxygen-18 and deuterium in river waters across the United States. *Hydrological processes*, 15(7), pp. 1363-1393.
- Kim, J.H. and Jackson, R.B., 2012. A global analysis of groundwater recharge for vegetation, climate, and soils. *Vadose Zone Journal*, 11(1), pp.0-0.

- Kirchner, J.W., 2016. Aggregation in environmental systems-Part 1: Seasonal tracer cycles quantify young water fractions, but not mean transit times, in spatially heterogeneous catchments. *Hydrology and Earth System Sciences*, 20(1), pp.279-297.
- Knoll, L., Breuer, L. and Bach, M., 2019. Large scale prediction of groundwater nitrate concentrations from spatial data using machine learning. *Science of the total environment*, 668, pp.1317-1327.
- Krishan, G., 2015. Environmental tracer techniques in groundwater investigations. *Water and Energy International*, 58(7), pp.57-63.
- Liaw A, Wiener M. 2002. Classification and Regression by randomForest. *R News* 2 (3): 18–22.
- Lindsey BD, Jurgens BC, Belitz K. 2019. Tritium as an Indicator of Modern, Mixed, and Premodern Groundwater Age. USGS: Scientific Investigations Report 2019-5090 1: 30.
- Maloszewski, P., Moser, H., Stichler, W., Bertleff, B. and Hedin, K., 1990. Modelling of groundwater pollution by river bank filtration using oxygen-18 data. *IAHS-AISH publication*, (173), pp.153-161.
- Marloth R. 1905. Results of further experiments on table mountain for ascertaining the amount of moisture deposited from the southeast clouds. *Transactions of the South African Philosophical Society* 16 (1): 97–105.
- McGuire, K.J. and McDonnell, J.J., 2006. A review and evaluation of catchment transit time modeling. *Journal of Hydrology*, 330(3-4), pp.543-563.
- McMahon PB, Plummer LN, Bohlke JK, Shapiro SD, Hinkle SR. 2011. A comparison of recharge rates in aquifers of the United States based on groundwater-age data. *Hydrogeology Journal* 19 (4): 779–800.

- From the New York State Education Department. Geology. Available from Geographic Information System: Surficial Geology Shape Files; accessed 1 April 2020.
- Ouedraogo I, Defourny P, Vanclooster M. 2019. Application of random forest regression and comparison of its performance to multiple linear regression in modeling groundwater nitrate concentration at the African continent scale. *Hydrogeology Journal* 27 (3): 1081-1098.
- Pebesma, E.J., 2004. Multivariable geostatistics in S: the gstat package. *Computers & Geosciences*, 30: 683-691.
- PRISM Climate Group. 2012. PRISM Climate Data.
- R Core Team. 2018. R: A language and environment for statistical computing.
- Sánchez-Murillo, R. and Birkel, C., 2016. Groundwater recharge mechanisms inferred from isoscapes in a complex tropical mountainous region. *Geophysical Research Letters*, 43(10), pp. 5060-5069.
- Schenectady Department of Water. 2018. Annual Drinking Water Quality Report.
- Scholl MA, Gingerich SB, Tribble GW. 2002. The influence of microclimates and fog on stable isotope signatures used in interpretation of regional hydrology: East Maui, Hawaii. *Journal of Hydrology* 264 (1–4): 170–184
- Sharp, Z., 2017. Principles of stable isotope geochemistry.
- Simpson, E.S., 1952. The ground-water resources of Schenectady County, New York: New York Water Power and Control Comm. Bull. GW-30.
- Stahl, M, Gehring, J, and Jameel, Y. 2020. Isotopic variation in groundwater across the conterminous U.S. – insight into hydrologic processes. *Hydrological Processes*: 13832.

- Strauch G, Al-Mashaikhi KS, Bawain A, Knöller K, Friesen J, Müller T. 2014. Stable H and O isotope variations reveal sources of recharge in Dhofar, Sultanate of Oman. *Isotopes in Environmental and Health Studies* 50 (4): 475–490
- Troch, P.A., Berne, A., Bogaart, P., Harman, C., Hilberts, A.G., Lyon, S.W., Paniconi, C., Pauwels, V.R., Rupp, D.E., Selker, J.S. and Teuling, A.J., 2013. The importance of hydraulic groundwater theory in catchment hydrology: The legacy of Wilfried Brutsaert and Jean-Yves Parlange. *Water Resources Research*, 49(9), pp.5099-5116.
- Vander Zanden, H.B., Soto, D.X., Bowen, G.J. and Hobson, K.A., 2016. Expanding the isotopic toolbox: applications of hydrogen and oxygen stable isotope ratios to food web studies. *Frontiers in Ecology and Evolution*, 4, p.20.
- Wassenaar LI, Van Wilgenburg SL, Larson K, Hobson KA. 2009. A groundwater isoscape (δD , $\delta^{18}O$) for Mexico. *Journal of Geochemical Exploration* 102 (3): 123–136.
- West JB, Bowen GJ, Dawson TE, Tu KP. 2010. *Isoscapes* (JB West, GJ Bowen, TE Dawson, and KP Tu, eds). Springer Netherlands: Dordrecht.
- Winslow, J.D., 1962. Effect of stream infiltration on ground-water temperatures near Schenectady, New York: U.S. Geological Survey Professional Paper 450—C, p. 125–128.
- Winslow, J.D., Stewart, H.G., Johnson, R.H. and Grain, L.J., 1965. Ground-water resources of eastern Schenectady County. *Bulletin*, 57.
- Zirchky, J., 1985. Geostatistics for environmental monitoring and survey design. *Environment international*, 11(6), pp.515-524.